Top Quark Interactions and the Search for New Physics

F. Larios[†] and C.–P. Yuan

Department of Physics and Astronomy, Michigan State University East Lansing, Michigan 48824, USA

Abstract

A complete characterization of all the possible effective interactions up to dimension 5 of the top and bottom quarks with the electroweak gauge bosons have been made within the context of the non-linear chiral Lagrangian. The dimension 5 operators (19 in total) can contribute to the $V_L V_L \to t\bar{t}$ or $t\bar{b}$ amplitudes with a leading energy power of E^3 (E^2) for fermion pairs with same (opposite) sign helicities. Because of the equivalence between the longitudinal weak boson and the corresponding would-be Goldstone boson in high energy collisions (Goldstone Equivalence Theorem), they are sensitive to the electroweak symmetry breaking sector. We also show the top quark production rates at the LHC and the LC via $V_L V_L$ fusion processes. At the LC, if no anomalous production rate is found, these coefficients can be bound (based on the naive dimensional analysis) to be of order 10^{-1} . This is about an order of magnitude more stringent than the bounds for the next-to-leading order bosonic operators commonly studied in $V_L V_L \to V_L V_L$ scatterings. The effects on a CP-odd observable are also briefly discussed.

PACS numbers: 14.65.Ha, 12.39.Fe, 12.60.-i

 $^{^\}dagger Also$ at the Departamento de Física, CINVESTAV, Ap
do. Postal 14-740, 07000 México, D.F., México.

1 Introduction

Despite the unquestionable significance of its achievements, like that of predicting the existence of the top quark, there is no reason to believe that the Standard Model (SM) is the final theory. For instance, the SM contains many arbitrary parameters with no apparent connections. In addition, the SM provides no satisfactory explanation for the symmetry-breaking mechanism which takes place and gives rise to the observed mass spectrum of the gauge bosons and fermions. Because the top quark is heavy relative to other observed fundamental particles, one expects that any underlying theory, to supersede the SM at some high energy scale $\Lambda \gg m_t$, will easily reveal itself at lower energies through the effective interactions of the top quark to other light particles. Also because the top quark mass $(\sim v/\sqrt{2})$ is of the order of the Fermi scale $v = (\sqrt{2}G_F)^{-1/2} = 246\,\mathrm{GeV}$ [1], which characterizes the electroweak symmetry-breaking scale, the top quark system could be a useful probe for the symmetry-breaking sector. Furthermore, the fermion mass generation can be closely related to the electroweak symmetry-breaking mechanism, one expects some residual effects of this mechanism to appear in accordance with the mass hierarchy [2, 3, 4]. This means that new effects should be more apparent in the top quark sector than in any other light sector of the theory. Therefore, it is important to study the top quark system as a direct tool to probe new physics effects [5].

Because of the great diversity of models proposed for possible new physics (beyond the SM), it has become necessary to study these possible new interactions in a model independent approach [6]. This approach has proved to render relevant non-trivial information about the possible deviations from the standard couplings of the heavier elementary particles (heavy scalar bosons, the bottom and the top quarks, etc.) [7]. Our study focuses on the top quark, which because of its remarkably higher mass is the best candidate among the fermion particles for manifesting these anomalous interactions at high energies.

A common approach to study these anomalous couplings is to consider the most general on-shell vertices (form factors) involving the bottom and the top quarks and the gauge bosons of interest [5]. In this work we will incorporate the effective chiral Lagrangian approach [8], which is based on the principle of gauge symmetry, but the symmetry is realized in the most general (non-linear) form so as to encompass all the possible interactions consistent with the existing experimental data. The idea of using this approach is to exploit the linearly realized $\mathrm{U}(1)_{\mathrm{em}}$ symmetry and the non-linearly realized $\mathrm{SU}(2)_{\mathrm{L}} \times \mathrm{U}(1)_{\mathrm{Y}}$ symmetry to make a systematic characterization of all the anomalous couplings. In this way, for example, different couplings which otherwise would be considered as independent become related through the equations of motion.

In Ref. [4] it was shown that low energy data (including Z pole physics) generally do not impose any stringent constraints on the κ coefficients of the anomalous

couplings in $\mathcal{L}^{(4)}$ [cf. Eq. (33)]. Hence these anomalous couplings have to be directly measured via production of top quarks at the colliders. For instance, the couplings $\kappa_{L,R}^{CC}$ can be measured from the decay of the top quarks in $t\bar{t}$ pairs produced either at hadron colliders, such as the Tevatron and the Large Hadron Collider (LHC), or at the electron linear collider (LC). They can also be studied from the production of the single-top quark events via W-gluon fusion ($Wg \to t\bar{b}$) [9, 10, 11, 12, 13] or the Drell-Yan like ($W^* \to t\bar{b}$) [14, 15] processes at the hadron colliders, as well as from the W-photon fusion ($W\gamma \to t\bar{b}$) process at the electron colliders [16]. The coupling $\kappa_{L,R}^{NC}$ can only be sensitively probed at a future linear collider via the $e^+e^- \to \gamma, Z \to t\bar{t}$ process [17] because at hadron colliders the $t\bar{t}$ production rate is dominated by QCD interactions ($q\bar{q}, gg \to t\bar{t}$). At the LHC $\kappa_{L,R}^{NC}$ may also be studied via the associated production of $t\bar{t}$ with Z bosons, which deserves a separate study.

In this work, we will extend the previous study by including dimension 5 fermionic operators, and then examine the precision with which the coefficients of these operators can be measured in high energy collisions. Since it is the electroweak symmetry breaking sector that we are interested in, we shall concentrate on the interaction of the top quark with the longitudinal weak gauge bosons; which are equivalent to the would-be Goldstone bosons in the high energy limit. This equivalence is known as the Goldstone Equivalence Theorem [18]-[21].

For simplicity, we will only construct the complete set of dimension 5 effective operators for the fermions t and b, although our results can be trivially extended for operators including other fermions such as the flavor changing neutral interactions t-c-Z, t-c- γ [22] and t-c-g [23].

Our strategy for probing these anomalous dimension 5 operators ($\mathcal{L}^{(5)}$) is to study the production of $t\bar{t}$ pairs as well as single-t or \bar{t} via the $W_L^+W_L^-$, Z_LZ_L and $W_L^\pm Z_L$ (denoted in general as V_LV_L) fusion processes in the TeV region. As we shall show later, the leading contribution of the scattering amplitudes at high energy goes as E^3 for the anomalous operators $\mathcal{L}^{(5)}$, where $E = \sqrt{s}$ is the CM energy of the W^+W^- or ZZ system (that produces $t\bar{t}$), or the $W^\pm Z$ system (that produces $t\bar{b}$ or $b\bar{t}$). On the other hand, when the coefficients $\kappa_{L,R}^{CC}$ and $\kappa_{L,R}^{NC}$ are zero, the dimension 4 operators $\mathcal{L}^{(4)}$ can at most contribute with the first power E^1 to these scattering V_LV_L processes. Hence, in this case, the $V_LV_L \to f\bar{f}'$ scatterings in the high energy region are more sensitive to $\mathcal{L}^{(5)}$ than to $\mathcal{L}^{(4)}$. If these κ 's are not zero, then the high energy behavior can at most grow as E^2 as compared to E^3 for the dimension 5 operators (See Appendix B).

As mentioned before, the dimension 4 anomalous couplings κ 's are better measured at the scale of M_W or m_t by studying the decay or the production of the top quark at either the Tevatron, the LHC, or the LC near the $t\bar{t}$ threshold. Since, as mentioned above, the dimension 5 operators are better measured in the TeV region, we shall assume that by the time their measurement is feasible, the κ 's will already be known. Thus, to simplify our discussion, we will take the values of the κ 's to be

zero when presenting our numerical results.

We show that there are 19 independent dimension 5 operators (with only t, b and gauge boson fields) in $\mathcal{L}^{(5)}$ after imposing the equations of motion for the effective chiral Lagrangian. It is expected that at the LHC or the LC there will be about a few hundreds to a few thousands of $t\bar{t}$ pairs or single-t (or single- \bar{t}) events produced via the V_LV_L fusion processes. The coefficients of these operators, with the pre-factor $\frac{1}{\Lambda}$, could be measured at the LC (less likely at the LHC) to order 10^{-2} or 10^{-1} . As will shown later, the pre-factor $\frac{1}{\Lambda}$ is suggested by the naive dimensional analysis [25], and Λ is the cut-off scale of the effective theory. It could be the lowest new heavy mass scale, or something around $4\pi v \simeq 3.1$ TeV if no new resonances exist below Λ . As a comparison, the coefficients of the NLO bosonic operators are usually determined to about an order of 10^{-1} or 1 via $V_LV_L \to V_LV_L$ processes [21, 24]. Hence, the scattering processes $V_LV_L \to t\bar{t}$, $t\bar{b}$, or $b\bar{t}$ at high energy may be more sensitive for probing some symmetry breaking mechanisms than $V_LV_L \to V_LV_L$.

This paper is organized as follows. In section 2 the general framework of the Electroweak Chiral Lagrangian is presented. In section 3 we make a systematic characterization of all the independent dimension 5 operators that are invariant under the symmetry of the gauge group. Section 4 deals with the CP properties of these interactions. In section 5 we make a general analysis of their potential contribution to the production cross section of top quarks according to their behavior at high energies. A very useful simplification is made by considering an approximate custodial symmetry in our set of operators; this is discussed in section 6. Section 7 contains the analytical results for the amplitudes of various $V_L V_L$ fusion processes; an approximate custodial symmetry is assumed here, but the general expressions can be found in Appendices B and C. Finally, in section 8 we discuss the values for the coefficients of these anomalous operators at which a significant signal can appear at both the LHC and the LC; also, we include an example of how one can measure possible CP violating effects coming from these operators. Section 9 has our conclusions.

2 The ingredients of the Electroweak Chiral Lagrangian

We consider the electroweak theories in which the gauge symmetry $G \equiv \mathrm{SU}(2)_L \times \mathrm{U}(1)_Y$ is spontaneously broken down to $H = \mathrm{U}(1)_{\mathrm{em}}[4, 25, 26, 27]$. There are three Goldstone bosons, ϕ^a (a = 1, 2, 3), generated by this breakdown of G into H, which are eventually eaten by the W^\pm and Z gauge bosons and become their longitudinal degrees of freedom.

In the non-linearly realized chiral Lagrangian formulation, the Goldstone bosons transform non-linearly under G but linearly under the subgroup H. A convenient

way to handle this is to introduce the matrix field

$$\Sigma = \exp\left(i\frac{\phi^a \tau^a}{v_a}\right) \,, \tag{1}$$

where τ^a , a=1,2,3 are the Pauli matrices normalized as $\text{Tr}(\tau^a\tau^b)=2\delta_{ab}$. The matrix field Σ transforms under G as

$$\Sigma \to \Sigma' = g_L \Sigma g_R^{\dagger}, \tag{2}$$

with

$$g_L = \exp\left(i\frac{\alpha^a \tau^a}{2}\right) ,$$

$$g_R^{\dagger} = \exp\left(-i\frac{y\tau^3}{2}\right) ,$$
(3)

where $\alpha^{1,2,3}$ and y are the group parameters of G. Because of the U(1)_{em} invariance, $v_1 = v_2 = v$ in Eq. (1), but they are not necessarily equal to v_3 . In the SM, v is the vacuum expectation value of the Higgs boson field, and characterizes the scale of the symmetry-breaking. Also, $v_3 = v$ arises from the approximate custodial symmetry present in the SM. It is this symmetry that is responsible for the tree-level relation

$$\rho = \frac{M_W^2}{M_Z^2 \cos^2 \theta_W} = 1 \tag{4}$$

in the SM, where θ_W is the electroweak mixing angle, M_W and M_Z are the masses of W^{\pm} and Z boson, respectively. In this paper we assume the underlying theory guarantees that $v_1 = v_2 = v_3 = v$.

In the context of this non-linear formulation of the electroweak theory, the massive charged and neutral weak bosons can be defined by means of the *composite* field:

$$W_{\mu}^{a} = -i \operatorname{Tr}(\tau^{a} \Sigma^{\dagger} D_{\mu} \Sigma) \tag{5}$$

where¹

$$D_{\mu}\Sigma = \left(\partial_{\mu} - ig\frac{\tau^{a}}{2}W_{\mu}^{a}\right)\Sigma . \tag{6}$$

Here, W^a_μ is the gauge boson associated with the $\mathrm{SU}(2)_L$ group, and its transformation is

$$\tau^{a}W_{\mu}^{a} \to \tau^{a}W_{\mu}^{'a} = g_{L} \tau^{a}W_{\mu}^{a} g_{L}^{\dagger} + \frac{2i}{g}g_{L}\partial_{\mu}g_{L}^{\dagger},$$
(7)

where g is the gauge coupling. The $D_{\mu}\Sigma$ term transforms under G as

$$D_{\mu}\Sigma \to D_{\mu}\Sigma' = g_L (D_{\mu}\Sigma) g_R^{\dagger} + g_L \Sigma \partial_{\mu} g_R^{\dagger} . \tag{8}$$

This is not the covariant derivative of Σ . The covariant derivative is $D_{\mu}\Sigma = \partial_{\mu}\Sigma - ig\frac{\tau^a}{2}W_{\mu}^a\Sigma + ig'\Sigma\frac{\tau^3}{2}B_{\mu}$, such that $D_{\mu}\Sigma \to D_{\mu}\Sigma' = g_L(D_{\mu}\Sigma)g_R^{\dagger}$.

Therefore, by using the commutation rules for the Pauli matrices and the fact that Tr(AB) = Tr(BA) we can prove that the composite field \mathcal{W}^a_μ will transform under G in the following manner:

$$\mathcal{W}^3_{\mu} \to \mathcal{W}'^3_{\mu} = \mathcal{W}^3_{\mu} - \partial_{\mu} y \,, \tag{9}$$

$$\mathcal{W}_{\mu}^{\pm} \to \mathcal{W}_{\mu}^{\prime \pm} = e^{\pm iy} \mathcal{W}_{\mu}^{\pm} , \qquad (10)$$

where

$$\mathcal{W}^{\pm}_{\mu} = \frac{\mathcal{W}^{1}_{\mu} \mp i\mathcal{W}^{2}_{\mu}}{\sqrt{2}} \,. \tag{11}$$

Also, it is convenient to define the field

$$\mathcal{B}_{\mu} = g' B_{\mu} , \qquad (12)$$

which is really the same gauge boson field associated with the $U(1)_Y$ group (g') is the gauge coupling). The field \mathcal{B}_{μ} transforms under G as

$$\mathcal{B}_{\mu} \to \mathcal{B}'_{\mu} = \mathcal{B}_{\mu} + \partial_{\mu} y \ . \tag{13}$$

We now introduce the composite fields \mathcal{Z}_{μ} and \mathcal{A}_{μ} as

$$\mathcal{Z}_{\mu} = \mathcal{W}_{\mu}^3 + \mathcal{B}_{\mu} , \qquad (14)$$

$$s_w^2 \mathcal{A}_{\mu} = s_w^2 \mathcal{W}_{\mu}^3 - c_w^2 \mathcal{B}_{\mu} \,, \tag{15}$$

where $s_w^2 \equiv \sin^2 \theta_W$, and $c_w^2 = 1 - s_w^2$. In the unitary gauge $(\Sigma = 1)$

$$W^a_\mu = -gW^a_\mu \ , \tag{16}$$

$$\mathcal{Z}_{\mu} = -\frac{g}{G_{\nu}} Z_{\mu} , \qquad (17)$$

$$\mathcal{A}_{\mu} = -\frac{e}{s_{\nu}^2} A_{\mu} , \qquad (18)$$

where we have used the relations $e = gs_w = g'c_w$, $W^3_{\mu} = c_w Z_{\mu} + s_w A_{\mu}$, and $B_{\mu} = -s_w Z_{\mu} + c_w A_{\mu}$. In general, the composite fields contain Goldstone boson fields:

$$\mathcal{Z}_{\mu} = -\frac{g}{c_{w}} Z_{\mu} + \frac{2}{v} \partial_{\mu} \phi^{3} - i \frac{2g}{v} (W_{\mu}^{+} \phi^{-} - W_{\mu}^{-} \phi^{+}) + i \frac{2}{v^{2}} (\phi^{-} \partial_{\mu} \phi^{+} - \phi^{+} \partial_{\mu} \phi^{-}) + \cdots,$$
(19)

$$W_{\mu}^{\pm} = -gW_{\mu}^{\pm} + \frac{2}{v}\partial_{\mu}\phi^{\pm} \pm i\frac{2g}{v}(\phi^{3}W_{\mu}^{\pm} - W_{\mu}^{3}\phi^{\pm}) \pm i\frac{2}{v^{2}}(\phi^{\pm}\partial_{\mu}\phi^{3} - \phi^{3}\partial_{\mu}\phi^{\pm}) + \cdots,$$
(20)

where \cdots denotes terms with 3 or more boson fields.

The transformations of \mathcal{Z}_{μ} and \mathcal{A}_{μ} under G are

$$\mathcal{Z}_{\mu} \to \mathcal{Z}'_{\mu} = \mathcal{Z}_{\mu} \,, \tag{21}$$

$$\mathcal{A}_{\mu} \to \mathcal{A}'_{\mu} = \mathcal{A}_{\mu} - \frac{1}{s_w^2} \partial_{\mu} y \ . \tag{22}$$

Hence, under G the fields \mathcal{W}_{μ}^{\pm} and \mathcal{Z}_{μ} transform as vector fields, but \mathcal{A}_{μ} transforms as a gauge boson field which plays the role of the photon field A_{μ} .

Using the fields defined as above, one may construct the $SU(2)_L \times U(1)_Y$ gauge invariant interaction terms in the chiral Lagrangian

$$\mathcal{L}^{B} = -\frac{1}{4g^{2}} \mathcal{W}^{a}_{\mu\nu} \mathcal{W}^{a\mu\nu} - \frac{1}{4g'^{2}} \mathcal{B}_{\mu\nu} \mathcal{B}^{\mu\nu} + \frac{v^{2}}{4} \mathcal{W}^{+}_{\mu} \mathcal{W}^{-\mu} + \frac{v^{2}}{8} \mathcal{Z}_{\mu} \mathcal{Z}^{\mu} + \dots,$$
(23)

where

$$W^{a}_{\mu\nu} = \partial_{\mu}W^{a}_{\nu} - \partial_{\nu}W^{a}_{\mu} + \epsilon^{abc}W^{b}_{\mu}W^{c}_{\nu} , \qquad (24)$$

$$\mathcal{B}_{\mu\nu} = \partial_{\mu}\mathcal{B}_{\nu} - \partial_{\nu}\mathcal{B}_{\mu} , \qquad (25)$$

and where \dots denotes other possible four- or higher-dimension operators [27]. It is easy to show that²

$$W_{\mu\nu}^a \tau^a = -g \Sigma^\dagger W_{\mu\nu}^a \tau^a \Sigma \tag{26}$$

and

$$\mathcal{W}^a_{\mu\nu}\mathcal{W}^{a\mu\nu} = g^2 W^a_{\mu\nu} W^{a\mu\nu} , \qquad (27)$$

which does not have any explicit dependence on Σ . This simply reflects the fact that the kinetic term is not related to the Goldstone bosons sector, i.e. it does not originate from the symmetry-breaking sector.

The mass terms in Eq. (23) can be expanded as

$$\frac{v^2}{4} W_{\mu}^{+} W^{-\mu} + \frac{v^2}{8} Z_{\mu} Z^{\mu} = \partial_{\mu} \phi^{+} \partial^{\mu} \phi^{-} + \frac{1}{2} \partial_{\mu} \phi^{3} \partial^{\mu} \phi^{3} + \frac{g^2 v^2}{4} W_{\mu}^{+} W^{\mu -} + \frac{g^2 v^2}{8 c_w^2} Z_{\mu} Z^{\mu} + \dots$$
(28)

At the tree-level, the mass of W^{\pm} boson is $M_W = gv/2$ and the mass of Z boson is $M_Z = gv/2c_w$.

Fermions can be included in this context by assuming that each flavor transforms under $G=\mathrm{SU}(2)_L\times\mathrm{U}(1)_Y$ as

$$f \to f' = e^{iyQ_f} f \,, \tag{29}$$

 $J \to J = e^{\tau}$ $\frac{1}{2} \text{ Use } \mathcal{W}^a_\mu \tau^a = -2i\Sigma^\dagger D_\mu \Sigma \text{ , and } [\tau^a, \tau^b] = 2i\epsilon^{abc}\tau^c.$

where Q_f is the electric charge of f. $(Q_f = \frac{2}{3} \text{ for the top, and } Q_f = -\frac{1}{3} \text{ for the bottom quark.})$

Out of the fermion fields f_1 , f_2 (two different flavors) and the Goldstone bosons matrix field Σ , the usual linearly realized fields Ψ can be constructed. For example, the left-handed fermions $[SU(2)_L$ doublet] are

$$\Psi_L \equiv \begin{pmatrix} \psi_1 \\ \psi_2 \end{pmatrix}_L = \Sigma F_L = \Sigma \begin{pmatrix} f_1 \\ f_2 \end{pmatrix}_L \tag{30}$$

with $Q_{f_1} - Q_{f_2} = 1$. One can easily show that Ψ_L transforms linearly under G as

$$\Psi_L \to \Psi_L' = g\Psi_L \,, \tag{31}$$

where $g = \exp(i\frac{\alpha^a \tau^a}{2}) \exp(iy\frac{Y}{2}) \in G$, and $Y = \frac{1}{3}$ is the hypercharge of the left handed quark doublet.

In contrast, linearly realized right-handed fermions Ψ_R [SU(2)_L singlet] simply coincide with F_R , i.e.,

$$\Psi_R \equiv \begin{pmatrix} \psi_1 \\ \psi_2 \end{pmatrix}_R = F_R = \begin{pmatrix} f_1 \\ f_2 \end{pmatrix}_R. \tag{32}$$

With these fields we can now construct the most general gauge invariant chiral Lagrangian that includes the electroweak couplings of the top quark up to dimension four [4].

$$\mathcal{L}^{(4)} = i\overline{t}\gamma^{\mu} \left(\partial_{\mu} + i\frac{2s_{w}^{2}}{3}\mathcal{A}_{\mu}\right) t + i\overline{b}\gamma^{\mu} \left(\partial_{\mu} - i\frac{s_{w}^{2}}{3}\mathcal{A}_{\mu}\right) b$$

$$-\frac{1}{2} \left(1 - \frac{4s_{w}^{2}}{3} + \kappa_{L}^{NC}\right) \overline{t_{L}}\gamma^{\mu} t_{L} \mathcal{Z}_{\mu} - \frac{1}{2} \left(\frac{-4s_{w}^{2}}{3} + \kappa_{R}^{NC}\right) \overline{t_{R}}\gamma^{\mu} t_{R} \mathcal{Z}_{\mu}$$

$$-\frac{1}{2} \left(-1 + \frac{2s_{w}^{2}}{3}\right) \overline{b_{L}}\gamma^{\mu} b_{L} \mathcal{Z}_{\mu} - \frac{s_{w}^{2}}{3} \overline{b_{R}}\gamma^{\mu} b_{R} \mathcal{Z}_{\mu}$$

$$-\frac{1}{\sqrt{2}} \left(1 + \kappa_{L}^{CC}\right) \overline{t_{L}}\gamma^{\mu} b_{L} \mathcal{W}_{\mu}^{+} - \frac{1}{\sqrt{2}} \left(1 + \kappa_{L}^{CC}^{\dagger}\right) \overline{b_{L}}\gamma^{\mu} t_{L} \mathcal{W}_{\mu}^{-}$$

$$-\frac{1}{\sqrt{2}} \kappa_{R}^{CC} \overline{t_{R}}\gamma^{\mu} b_{R} \mathcal{W}_{\mu}^{+} - \frac{1}{\sqrt{2}} \kappa_{R}^{CC}^{\dagger} \overline{b_{R}}\gamma^{\mu} t_{R} \mathcal{W}_{\mu}^{-}$$

$$-m_{t} \overline{t} t - m_{b} \overline{b} b . \tag{33}$$

In the above equation, the coefficients $\kappa_L^{\rm NC}$, $\kappa_R^{\rm NC}$, $\kappa_L^{\rm CC}$, and $\kappa_R^{\rm CC}$ parametrize possible deviations from the SM predictions [4].

The constraints on the κ 's from the LEP/SLC data and from the recent measurement on $\operatorname{Br}(b \to s \gamma)$ [28], are given in Refs. [4] and [29], respectively. (We shall come back to these constraints later in the section of Conclusions.) As mentioned in the Introduction, in this paper we are setting these κ coefficients to be zero in $\mathcal{L}^{(4)}$, which will be denoted as $\mathcal{L}_{SM}^{(4)}$ from now on.

In the next section we will construct the complete set of independent operators of dimension 5, such that the complete effective Lagrangian relevant to this work will be

$$\mathcal{L}_{eff} = \mathcal{L}^B + \mathcal{L}_{SM}^{(4)} + \mathcal{L}^{(5)},$$
 (34)

where $\mathcal{L}^{(5)}$ denotes the higher dimensional operators.

3 Dimension five operators

Our next task is to find all the possible dimension five hermitian interactions that involve the top quark and the fields W_{μ}^{\pm} , \mathcal{Z}_{μ} and \mathcal{A}_{μ} . Notice that the gauge transformations associated with these and the composite fermion fields (Eq. (29)) are dictated simply by the U(1)_{em} group. We will follow a procedure similar to the one in Ref. [30], which consists of constructing all possible interaction terms that satisfy the required gauge invariance, and that are not equivalent to each other. The criterion for equivalence is based on the equations of motion (see Appendix A) and on partial integration. As for the five dimensions in these operators, three will come from the fermion fields, and the other two will involve the gauge bosons. To make a clear and systematic characterization, let us recognize the only three possibilities for these two dimensions:

- (1) Operators with two boson fields.
- (2) Operators with one boson field and one derivative.
- (3) Operators with two derivatives.
- (1) **Two boson fields.** First of all, notice that the \mathcal{A}_{μ} field gauge transformation (Eq. (22)) will restrict the use of this field to covariant derivatives only. Therefore, except for the field strength term $\mathcal{A}_{\mu\nu}$ only the \mathcal{Z} and \mathcal{W} fields can appear multiplying the fermions in any type of operators. Also, the only possible Lorentz structures are given in terms of $g_{\mu\nu}$ and $\sigma_{\mu\nu}$ tensors. We do not need to consider the tensor product of γ_{μ} 's since

$$\not a \not b = g_{\mu\nu} a^{\mu} b^{\nu} - i \sigma_{\mu\nu} a^{\mu} b^{\nu} . \tag{35}$$

Finally, we are left with only three possible combinations:

- (1.1) two \mathcal{Z}_{μ} 's,
- (1.2) two \mathcal{W}_{μ} 's, and
- (1.3) one of each.

Let us write down the corresponding operators for each case:

(1.1) Since $\sigma_{\mu\nu}$ is antisymmetric, only the $g_{\mu\nu}$ part is non-zero:³

$$O_{g\mathcal{Z}\mathcal{Z}} = \bar{t}_L t_R \mathcal{Z}_\mu \mathcal{Z}^\mu + h.c. \tag{36}$$

³ In the next section we will write explicitly the h.c. parts.

(1.2) Here, the antisymmetric part is non-zero too:

$$O_{qWW} = \bar{t}_L t_R W_{\mu}^+ W^{-\mu} + h.c. \tag{37}$$

$$O_{\sigma WW} = \bar{t}_L \sigma^{\mu\nu} t_R W_{\mu}^+ W_{\nu}^- + h.c. \tag{38}$$

(1.3) In this case we have two different quark fields, therefore we can distinguish two different combinations of chiralities:

$$O_{gWZL(R)} = \bar{t}_{L(R)}b_{R(L)}W_{\mu}^{+}Z^{\mu} + h.c.$$
(39)

$$O_{\sigma \mathcal{W} \mathcal{Z} L(R)} = \bar{t}_{L(R)} \sigma^{\mu \nu} b_{R(L)} \mathcal{W}_{\mu}^{+} \mathcal{Z}_{\nu} + h.c. \tag{40}$$

- (2) One boson field and one derivative. The obvious distinction arises:
- (2.1) the derivative acting on a fermion field, and
- (2.2) the derivative acting on the boson.
- (2.1) From Eqs. (22) and (29), the covariant derivative for the fermions is given by 4

$$D_{\mu}f = (\partial_{\mu} + iQ_{f}s_{w}^{2}\mathcal{A}_{\mu})f,$$

$$\overline{D_{\mu}f} = \bar{f}(\overleftarrow{\partial}_{\mu} - iQ_{f}s_{w}^{2}\mathcal{A}_{\mu}).$$
(41)

Notice that it depends on the fermion charge Q_f , hence the covariant derivative for the top quark is not the same as for the bottom quark; partial integration could not relate two operators involving derivatives on different quarks. Furthermore, by looking at the equations of motion we can immediately see, for example, that operators of the form $\bar{f} \not\subset \mathcal{D} f$ or $\bar{f}^{(up)} \not \mathcal{W}^+ \mathcal{D} f^{(down)}$ are equivalent to operators with two bosons, which have all been considered already. Following the latter statement and bearing in mind the identity of Eq. (35) we can see that only one Lorentz structure needs to be considered here, either one with $\sigma_{\mu\nu}$ or one with $g_{\mu\nu}$. Let us choose the latter.

$$O_{\mathcal{W}DbL(R)} = \mathcal{W}^{+\mu} \bar{t}_{L(R)} D_{\mu} b_{R(L)} + h.c. \tag{42}$$

$$O_{\mathcal{W}DtR(L)} = \mathcal{W}^{-\mu} \bar{b}_{L(R)} D_{\mu} t_{R(L)} + h.c. \tag{43}$$

$$O_{\mathcal{Z}Df} = \mathcal{Z}^{\mu} \bar{t}_L D_{\mu} t_R + h.c. \tag{44}$$

Of course, the \mathcal{A} field did not appear. Remember that its gauge transformation prevents us from using it on anything that is not a covariant derivative or a field strength $\mathcal{A}_{\mu\nu}$.

⁴To simplify notation we will use the same symbol D_{μ} for all covariant derivatives. Identifying which derivative we are referring to should be straightforward, e.g. D_{μ} in Eq. (41) is different from D_{μ} in Eq. (6).

(2.2) Since W transforms as a field with electric charge one, the covariant derivative is simply given by (see Eq. (10)):

$$D_{\mu}\mathcal{W}_{\nu}^{+} = (\partial_{\mu} + is_{w}^{2}\mathcal{A}_{\mu})\mathcal{W}_{\nu}^{+}$$

$$D_{\mu}^{\dagger}\mathcal{W}_{\nu}^{-} = (\partial_{\mu} - is_{w}^{2}\mathcal{A}_{\mu})\mathcal{W}_{\nu}^{-}$$

$$(45)$$

Obviously, since the neutral \mathcal{Z} field is invariant under the G group transformations [cf. Eq. (21)], we could always add it to our covariant derivative:

$$D_{\mu}^{(\mathcal{Z})} \mathcal{W}_{\nu}^{+} = (\partial_{\mu} + is_{w}^{2} \mathcal{A}_{\mu} + ia \mathcal{Z}_{\mu}) \mathcal{W}_{\nu}^{+}$$

where a would stand for any complex constant. Actually, considering this second derivative would insure the generality of our analysis, since for example by setting $a = c_w^2$ and comparing with Eqs. (14) and (15) we would automatically include the field strength term⁵

$$W_{\mu\nu}^{\pm} = \partial_{\mu}W_{\nu}^{\pm} - \partial_{\nu}W_{\mu}^{\pm} \pm i(W_{\mu}^{\pm}W_{\nu}^{3} - W_{\nu}^{3}W_{\mu}^{\pm}) = D_{\mu}^{(\mathcal{Z})}W_{\nu}^{\pm} - D_{\nu}^{(\mathcal{Z})}W_{\mu}^{\pm}. \tag{46}$$

However, this extra term in the covariant derivative would only be redundant. We can always decompose any given operator written in terms of $D_{\mu}^{(\mathcal{Z})}$ into the sum of the same operator in terms of the original D_{μ} plus another operator of the form $O_{gWZL(R)}$ or $O_{\sigma WZL(R)}$ [cf. Eqs. (39) and (40)]. Therefore, we only need to consider the covariant derivative (45) for the charged boson and still maintain the generality of our characterization. For the neutral \mathcal{Z} boson, the covariant derivative is just the ordinary one,

$$D_{\mu}\mathcal{Z}_{\nu} = \partial_{\mu}\mathcal{Z}_{\nu}. \tag{47}$$

The case for the \mathcal{A} boson is nevertheless different. Being the field that makes possible the U(1)_{em} covariance in the first place, it cannot be given any covariant derivative itself. For \mathcal{A} , we have the field strength:

$$\mathcal{A}_{\mu\nu} = \partial_{\mu}\mathcal{A}_{\nu} - \partial_{\nu}\mathcal{A}_{\mu} ,$$

Finally, we can now write the operators with the covariant derivative-on-boson terms. Unfortunately, no equations of motion can help us reduce the number of independent operators in this case, and we have to bring up both the $\sigma_{\mu\nu}$ and the $g_{\mu\nu}$ Lorentz structures.

$$O_{\sigma D \mathcal{Z}} = \bar{t}_L \sigma^{\mu\nu} t_R \partial_{\mu} \mathcal{Z}_{\nu} + h.c. \tag{48}$$

$$O_{gDZ} = \bar{t}_L t_R \partial_\mu \mathcal{Z}^\mu + h.c. \tag{49}$$

$$O_{\sigma DWL(R)} = \bar{t}_{L(R)} \sigma^{\mu\nu} b_{R(L)} D_{\mu} W_{\nu}^{+} + h.c.$$
 (50)

$$O_{gDWL(R)} = \bar{t}_{L(R)} b_{R(L)} D_{\mu} W^{+\mu} + h.c.$$
 (51)

$$O_{\mathcal{A}} = \bar{t}_L \sigma^{\mu\nu} t_R \mathcal{A}_{\mu\nu} + h.c. \tag{52}$$

⁵From Eqs. (11) and (24), we write $W^{\pm}_{\mu\nu} = \frac{1}{\sqrt{2}} (W^1_{\mu\nu} \mp iW^2_{\mu\nu}).$

(3) Operators with two derivatives.

As it turns out, all operators of this kind are equivalent to the ones already given in the previous cases. Here, we shall present the argument of why this is so. First of all, we only have two possibilities:

- (3.1) one derivative acting on each fermion field, and
- (3.2) both derivatives acting on the same fermion field.
- (3.2) Again, by using the equations of motion twice we can relate the operator $\bar{f} \mathcal{D} \mathcal{D} f$ to operators of the type (1.1), (1.2) or (1.3). Either $\bar{f} \sigma^{\mu\nu} D_{\mu} D_{\nu} f$, or $\bar{f} D^{\mu} D_{\mu} f$ needs to be considered. This time we choose the former, which can be proved to be nothing but the operator $O_{\mathcal{A}}$ itself, i.e. Eq. (52). ⁶.

4 Hermiticity and CP invariance

The above list of the dimension 5 operators is complete in the sense that it includes all non-equivalent dimension five interaction terms that satisfy $\mathrm{SU}(2)_L \times \mathrm{U}(1)_Y$ gauge invariance. It is convenient now to analyze their CP properties. In order to make our study more systematic and clear we will re-write this list again, but this time we will display the added hermitian conjugate part in detail. By doing this the CP transformation characteristics will be most clearly presented too.

Let us divide the list of operators in two: those with only the top quark, and those involving both top and bottom quarks.

4.1 Interactions with top quarks only

Let's begin by considering the operator O_{gZZ} . We will include an arbitrary constant coefficient a which in principle could be complex, then

$$O_{gZZ} \sim a\bar{t}_L t_R \mathcal{Z}_{\mu} \mathcal{Z}^{\mu} + a^* \bar{t}_R t_L \mathcal{Z}_{\mu} \mathcal{Z}^{\mu}$$

= $Re(a)\bar{t}t \mathcal{Z}_{\mu} \mathcal{Z}^{\mu} + Im(a)i\bar{t}\gamma_5 t \mathcal{Z}_{\mu} \mathcal{Z}^{\mu}$.

⁶This can be easily checked by applying the definition of D_{μ} in Eq. (41).

Our hermitian operator has naturally split into two independent parts: one that preserves parity (scalar), and one that does not (pseudoscalar). Also, the first part is CP even whereas the second one is odd. The natural separation of these two parts happens to be a common feature of all operators with only one type of fermion field. Nevertheless, not always will the parity conserving part also be CP even, as we shall soon see.

Below, the complete list of all 7 operators with only the top quark is given. In all cases the two independent terms are included; the first one is CP even, and the second one is CP odd. They are:

$$O_{g\mathcal{Z}\mathcal{Z}} = \frac{1}{\Lambda} Re(a_{zz1}) \bar{t} t \mathcal{Z}_{\mu} \mathcal{Z}^{\mu} + \frac{1}{\Lambda} Im(a_{zz1}) i \bar{t} \gamma_5 t \mathcal{Z}_{\mu} \mathcal{Z}^{\mu}, \tag{53}$$

$$O_{gWW} = \frac{1}{\Lambda} Re(a_{ww1}) \bar{t} t W_{\mu}^{+} W^{-\mu} + \frac{1}{\Lambda} Im(a_{ww1}) i \bar{t} \gamma_5 t W_{\mu}^{+} W^{-\mu}, \qquad (54)$$

$$O_{\sigma WW} = \frac{1}{\Lambda} Im(a_{ww2}) i\bar{t}\sigma^{\mu\nu} t \mathcal{W}_{\mu}^{+} \mathcal{W}_{\nu}^{-} + \frac{1}{\Lambda} Re(a_{ww2}) \bar{t}\sigma^{\mu\nu} \gamma_5 t \mathcal{W}_{\mu}^{+} \mathcal{W}_{\nu}^{-}, \qquad (55)$$

$$O_{\mathcal{Z}Df} = \frac{1}{\Lambda} Im(a_{z3}) i\bar{t} D_{\mu} t \mathcal{Z}^{\mu} + \frac{1}{\Lambda} Re(a_{z3}) \bar{t} \gamma_5 D_{\mu} t \mathcal{Z}^{\mu}, \tag{56}$$

$$O_{gDZ} = \frac{1}{\Lambda} Im(a_{z4}) i \bar{t} \gamma_5 t \partial_{\mu} \mathcal{Z}^{\mu} + \frac{1}{\Lambda} Re(a_{z4}) \bar{t} t \partial_{\mu} \mathcal{Z}^{\mu}, \tag{57}$$

$$O_{\sigma D \mathcal{Z}} = \frac{1}{\Lambda} Re(a_{z2}) \bar{t} \sigma^{\mu\nu} t \partial_{\mu} \mathcal{Z}_{\nu} + \frac{1}{\Lambda} Im(a_{z2}) i \bar{t} \sigma^{\mu\nu} \gamma_5 t \partial_{\mu} \mathcal{Z}_{\nu}, \tag{58}$$

$$O_{\mathcal{A}} = \frac{1}{\Lambda} Re(a_{\mathcal{A}}) \bar{t} \sigma^{\mu\nu} t \mathcal{A}_{\mu\nu} + \frac{1}{\Lambda} Im(a_{\mathcal{A}}) i\bar{t} \sigma^{\mu\nu} \gamma_5 t \mathcal{A}_{\mu\nu}. \tag{59}$$

Notice that in the operator O_{gDZ} the CP even part happens to be parity violating. This is because under a CP transformation a scalar term $\bar{t}t$ remains intact, i.e. it does not change sign, whereas a pseudoscalar term $\bar{t}\gamma_5 t$ changes sign. Also, the gauge bosons change sign under C, which is what makes the scalar part of the O_{gDZ} operator to change sign under CP. On the contrary, the operator O_{gZZ} contains two bosons; thus two changes of sign that counteract each other. Therefore, it is the scalar part of O_{gZZ} that is CP even. In Table 1 we summarize in detail the discrete C, P and CP symmetries of the above operators.

As for the size of these effective operators, based on the naive dimensional analysis (NDA) their coefficients are of order $\frac{1}{\Lambda}$, where Λ is the cut-off scale of the effective theory. Therefore, the natural size of the normalized coefficients (the a's) is of order one.

4.2 Interactions with both top and bottom quarks

Below, we show the next list of 12 operators with both top and bottom quarks.⁷ Again, we include an arbitrary complex coefficient a. They are:

$$O_{gWZL(R)} = \frac{1}{\Lambda} a_{wz1L(R)} \bar{t}_{L(R)} b_{R(L)} W_{\mu}^{+} \mathcal{Z}^{\mu} + \frac{1}{\Lambda} a_{wz1L(R)}^{*} \bar{b}_{R(L)} t_{L(R)} W_{\mu}^{-} \mathcal{Z}^{\mu}, \qquad (60)$$

$$O_{\sigma W Z L(R)} = \frac{1}{\Lambda} a_{wz2L(R)} \bar{t}_{L(R)} \sigma^{\mu\nu} b_{R(L)} \mathcal{W}_{\mu}^{+} \mathcal{Z}_{\nu} + \frac{1}{\Lambda} a_{wz2L(R)}^{*} \bar{b}_{R(L)} \sigma^{\mu\nu} t_{L(R)} \mathcal{W}_{\mu}^{-} \mathcal{Z}_{\nu}, (61)$$

$$O_{WDbL(R)} = \frac{1}{\Lambda} a_{bw3L(R)} \mathcal{W}^{+\mu} \bar{t}_{L(R)} D_{\mu} b_{R(L)} + \frac{1}{\Lambda} a_{bw3L(R)}^* \mathcal{W}^{-\mu} \overline{D_{\mu} b_{R(L)}} t_{L(R)}, \quad (62)$$

$$O_{WDtR(L)} = \frac{1}{\Lambda} a_{w3R(L)} W^{-\mu} \bar{b}_{L(R)} D_{\mu} t_{R(L)} + \frac{1}{\Lambda} a_{w3R(L)}^* W^{+\mu} \overline{D_{\mu}} t_{R(L)} b_{L(R)}, \tag{63}$$

$$O_{\sigma D \mathcal{W} L(R)} = \frac{1}{\Lambda} a_{w2L(R)} \bar{t}_{L(R)} \sigma^{\mu\nu} b_{R(L)} D_{\mu} \mathcal{W}_{\nu}^{+} + \frac{1}{\Lambda} a_{w2L(R)}^{*} \bar{b}_{R(L)} \sigma^{\mu\nu} t_{L(R)} D_{\mu}^{\dagger} \mathcal{W}_{\nu}^{-}, (64)$$

$$O_{gDWL(R)} = \frac{1}{\Lambda} a_{w4L(R)} \bar{t}_{L(R)} b_{R(L)} D_{\mu} \mathcal{W}^{+\mu} + \frac{1}{\Lambda} a_{w4L(R)}^* \bar{b}_{R(L)} t_{L(R)} D_{\mu}^{\dagger} \mathcal{W}^{-\mu}.$$
 (65)

In this case, if a is real $(a = a^*)$ then $O_{gWZL(R)}$ and $O_{\sigma DWL(R)}$ are both CP even, but $O_{\sigma WZL(R)}$, $O_{WDbL(R)}$, $O_{WDtR(L)}$ and $O_{gDWL(R)}$ are odd. Just the other way around if a is purely imaginary [cf. Table 1].

The dimension five Lagrangian $\mathcal{L}^{(5)}$ is simply the sum of all these 19 operators (Eqs. (53) to (65)), i.e.

$$\mathcal{L}^{(5)} = \sum_{i=1,19} O_i \tag{66}$$

For the purpose of this study; to estimate the possible effects on the production rates of top quarks in high energy collisions, only the CP conserving parts, which give imaginary vertices (as the SM ones), are relevant. This is because the amplitude squared depends linearly on the CP even terms, but only quadratically on the CP odd terms, and the *no-Higgs* SM ($\mathcal{L}_{SM}^{(4)}$) interactions⁸ are CP even when ignoring the CP-violating phase in the CKM quark mixing matrix.

However, this does not mean that we cannot probe the CP violating sector; as a matter of fact, later on in the section of Numerical Results we will show one observable that depends linearly on the CP odd coefficients. From now on, the appropriate CP even part (either real or imaginary) is assumed for each coefficient. To simplify notation we will use the same label; a_{zz1} will stand for $Re(a_{zz1})$, $a_{wz2L(R)}$ will stand for $Im(a_{wz2L(R)})$, and so on. The only exception will be a_A , whose real part is recognized as proportional to the magnetic moment of the top quark, and will be denoted by a_m . It is thus understood that all coefficients below are real numbers.

In conclusion, the dimension 5 Lagrangian consists of 19 independent operators which are listed from Eq. (53) to Eq. (65). Their eigenvalues under the C, P

⁷ $\overline{D_{\mu}f}_{R(L)}$ stands for $(D_{\mu}f_{R(L)})^{\dagger}\gamma_0$; $\bar{f}_{R(L)}$ stands for $(f_{R(L)})^{\dagger}\gamma_0$.

⁸Since in the unitary gauge $\mathcal{L}_{SM}^{(4)}$ reproduces the SM without the physical Higgs boson, we will refer to it as the *no-Higgs* SM.

and CP transformations are conveniently listed in Table 1. Operators with top and bottom quarks (right hand side of the Table), which are given in terms of the chiral components, are not eigenvectors of the C nor P transformations; therefore, only the CP eigenvalues are given.

Since the top quark is heavy, its mass of the order of the weak scale, it is likely that it will interact strongly with the Goldstone bosons which are equivalent to the longitudinal weak gauge bosons in the high energy regime. In the rest of this paper, we shall study how to probe these anomalous couplings from the production of top quarks via the $V_L V_L$ fusion process, where V_L stands for the longitudinally polarized W^{\pm} or Z bosons.

Operator		С	Р	CP		Operator		
O_{gDZ}	$i\bar{t}\gamma_5 t\partial_\mu \mathcal{Z}^\mu$	_	_	+	$O_{gDWL(R)}$	$i\bar{t}_{L(R)}b_{R(L)}D_{\mu}\mathcal{W}^{+\mu} + h.c.$	+	
	$ar{t}t\partial_{\mu}\mathcal{Z}^{\mu}$	_	+	_	, ,	$\bar{t}_{L(R)}b_{R(L)}D_{\mu}\mathcal{W}^{+\mu} + h.c.$	_	
$O_{\sigma D \mathcal{Z}}$	$ar{t}\sigma^{\mu u}t\partial_{\mu}\mathcal{Z}_{ u}$	+	+	+	$O_{\sigma DWL(R)}$	$\bar{t}_{L(R)}\sigma^{\mu\nu}b_{R(L)}D_{\mu}\mathcal{W}^{+}_{\nu} + h.c.$	+	
	$i\bar{t}\sigma^{\mu\nu}\gamma_5 t\partial_\mu \mathcal{Z}_\nu$	+	_	_		$i\bar{t}_{L(R)}\sigma^{\mu\nu}b_{R(L)}D_{\mu}\mathcal{W}^{+}_{\nu} + h.c.$	_	
O_{ZDf}	$i \bar{t} D_{\mu} t \mathcal{Z}^{\mu}$	+	+	+	$O_{WDtR(L)}$	$i\mathcal{W}^{-\mu}\overline{b}_{L(R)}D_{\mu}t_{R(L)} + h.c.$	+	
	$ar{t}\gamma_5 D_\mu t \mathcal{Z}^\mu$	+	_	_		$\mathcal{W}^{-\mu}\bar{b}_{L(R)}D_{\mu}t_{R(L)} + h.c.$	_	
O_{gZZ}	$ar{t}t\mathcal{Z}_{\mu}\mathcal{Z}^{\mu}$	+	+	+	$O_{WDbL(R)}$	$i\mathcal{W}^{+\mu}\bar{t}_{L(R)}D_{\mu}b_{R(L)} + h.c.$	+	
	$i ar{t} \gamma_5 t \mathcal{Z}_{\mu} \mathcal{Z}^{\mu}$	+	_	_		$\mathcal{W}^{+\mu}\bar{t}_{L(R)}D_{\mu}b_{R(L)} + h.c.$	_	
O_{gWW}	$ar{t}t\mathcal{W}_{\mu}^{+}\mathcal{W}^{-\mu}$	+	+	+	$O_{gWZL(R)}$	$\bar{t}_{L(R)}b_{R(L)}\mathcal{W}_{\mu}^{+}\mathcal{Z}^{\mu}+h.c.$	+	
	$i ar{t} \gamma_5 t \dot{\mathcal{W}}_{\mu}^+ \mathcal{W}^{-\mu}$	+	_	_		$i\bar{t}_{L(R)}b_{R(L)}\mathcal{W}_{\mu}^{+}\mathcal{Z}^{\mu}+h.c.$	_	
$O_{\sigma WW}$	$i\bar{t}\sigma^{\mu\nu}t\dot{\mathcal{W}}_{\mu}^{+}\mathcal{W}_{\nu}^{-}$	+	+	+	$O_{\sigma W \mathcal{Z}L(R)}$	$i\bar{t}_{L(R)}\sigma^{\mu\nu}b_{R(L)}W_{\mu}^{+}\mathcal{Z}_{\nu} + h.c.$	+	
	$\bar{t}\sigma^{\mu\nu}\gamma_5t\dot{\mathcal{W}}^+_{\mu}\mathcal{W}^{\nu}$	+	_	_		$\bar{t}_{L(R)}\sigma^{\mu\nu}b_{R(L)}\mathcal{W}_{\mu}^{+}\mathcal{Z}_{\nu} + h.c.$	_	
$O_{\mathcal{A}}$	$\bar{t}\sigma^{\mu\nu}t\dot{\mathcal{A}}_{\mu\nu}$	+	+	+	_	_		
	$i\bar{t}\sigma^{\mu\nu}\gamma_5t\mathcal{A}_{\mu\nu}$	+	_	_				

Table 1: The C, P and CP eigenvalues of all the dimension 5 operators.

5 Probing the anomalous couplings

In the following sections, we shall study the production rates of $t\bar{t}$ ($t\bar{b}$ or $b\bar{t}$) from $W_L^+W_L^-$ or Z_LZ_L ($W_L^+Z_L$ or $W_L^-Z_L$) fusion processes in the TeV regime for both the LHC and the LC.

Before giving our analytical results (summarized in Appendices B and C), we shall estimate the expected sizes of these tree level amplitudes according to their high energy behavior. A general power counting rule has been given that estimates the

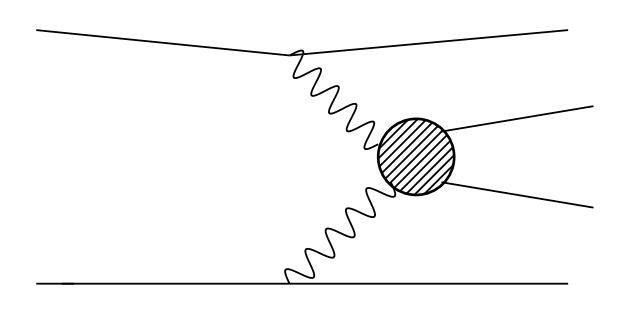


Figure 1: Production of $t\bar{t}$ ($t\bar{b}$ or $b\bar{t}$) from the V_LV_L fusion process.

high energy behavior of any amplitude T [31] as:

$$T = c_T v^{D_T} \left(\frac{v}{\Lambda}\right)^{N_{\mathcal{O}}} \left(\frac{E}{v}\right)^{D_{E0}} \left(\frac{E}{4\pi v}\right)^{D_{EL}} \left(\frac{M_W}{E}\right)^{e_v} H\left(\ln(E/\mu)\right)$$

$$D_{E0} = 2 + \sum_n \mathcal{V}_n (d_n + \frac{1}{2}f_n - 2) , \quad D_{EL} = 2L ,$$

$$(67)$$

where $D_T=4-e=0$ (e is the number of external lines, 4 in our case), $N_{\mathcal{O}}=0$ for all dimension 4 operators and $N_{\mathcal{O}}=1$ for all dimension 5 operators based upon the naive dimensional analysis (NDA) [25], $^9L=0$ is the number of loops in the diagrams, $H\left(\ln(E/\mu)\right)=1$ comes from the loop terms (none in our case), e_v accounts for any external v_{μ} -lines (none in our case of $V_L V_L \to t \bar{t}, \ t \bar{b}$), $^{10} \mathcal{V}_n$ is the number of vertices of type n that contain d_n derivatives and f_n fermionic lines. The dimensionless coefficient c_T contains possible powers of gauge couplings (g,g') and Yukawa couplings (y_f) from the vertices of the amplitude T, which can be directly counted.

One important remark about the above formula is that it cannot be directly applied to diagrams with external longitudinal V_L lines. As explained in Ref. [31], a significant part of the high energy behavior from diagrams with external V_L lines is cancelled when one adds all the relevant Feynman diagrams of the process; this is just a consequence of the gauge symmetry of the Lagrangian. To correctly apply Eq. (67), one has to make use of the Equivalence Theorem, and write down the relevant diagrams with the corresponding would-be Goldstone bosons. Then, the true high energy behavior will be given by the leading diagram. (If there is more than one leading diagram, there could be additional cancellations).

Let us analyze the high energy behavior of the $Z_L Z_L \to t\bar{t}$ process in the context of the dimension 4 couplings $\mathcal{L}^{(4)}$, as defined in Eq. 33. In Fig. 2 we show the

⁹ NDA counts Σ as Λ^0 , D_{μ} as $\frac{1}{\Lambda}$, and fermion fields as $\frac{1}{v\sqrt{\Lambda}}$. Hence, W^{\pm} , Z and A are also counted as $\frac{1}{\Lambda}$. After this counting, one should multiply the result by $v^2\Lambda^2$. Notice that up to the order of intent, the kinetic term of the gauge boson fields and the mass term of the fermion fields are two exceptions to the NDA, and are of order Λ^0 .

 $^{^{10}}$ v_{μ} is equal to $\epsilon_{\mu}^{(0)} - \frac{k_{\mu}}{M_{V}}$, where k_{μ} is the momentum of the gauge boson with mass M_{V} and $\epsilon_{\mu}^{(0)}$ is its longitudinal polarization vector.

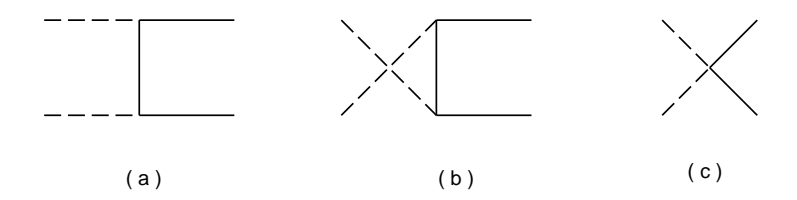


Figure 2: The corresponding Goldstone boson diagrams for $Z_L Z_L \to t\bar{t}$, i.e. $\phi^0 \phi^0 \to t\bar{t}$.

corresponding Goldstone boson diagrams, i.e. $\phi^0\phi^0 \to t\bar{t}$. The ϕ^0 -t-t vertex contains a derivative that comes from the expansion of the composite fields [cf. Eq. (19)], and the associated $(d_n + \frac{1}{2}f_n - 2)$ factor is $d_n + \frac{1}{2}f_n - 2 = 1 + \frac{1}{2}2 - 2 = 0$. This means $D_{E0} = 2$ for diagrams 2(a) and 2(b); both grow as E^2 at high energies. The four point vertex for diagram 2(c) can come from the mass term of the top quark or the second order terms from the expansion of \mathcal{Z}_{μ} in the effective Lagrangian. The ϕ^0 - ϕ^0 -t- \bar{t} vertex that comes from the mass term $m_t\bar{t}t$ does not contain any derivatives, hence the high energy behavior from this term goes like E^1 . The vertex that comes from the second order expansion of a term like $\bar{t}\gamma^{\mu}t\mathcal{Z}_{\mu}$ contains one derivative, and the corresponding amplitude 2(c) grows as E^2 in the high energy region. The conclusion is that diagram 2(c) behaves like E^2 as well. Seeing that there is more than one leading diagram we can suspect that there may be additional cancellations. How can we then obtain the correct high energy behavior for the Goldstone boson scattering amplitudes?

To answer this question let us use an alternative non-linear parametrization that is equivalent to $\mathcal{L}_{SM}^{(4)}$ (Eq. (33) with the κ 's equal zero), in the sense that it produces the exact same matrix elements [8], but with the advantage that the couplings of the fermions with the Goldstone bosons do not contain derivatives. We can rewrite the sum of \mathcal{L}^{B} [cf. Eq. (23)] and $\mathcal{L}_{SM}^{(4)}$ as:

$$\mathcal{L}_{SM} \equiv \mathcal{L}_{SM}^{(4)} + \mathcal{L}^{B} = \overline{\Psi}_{L} i \gamma^{\mu} D_{\mu}^{L} \Psi_{L} + \overline{\Psi}_{R} i \gamma^{\mu} D_{\mu}^{R} \Psi_{R} - \left(\overline{\Psi}_{L} \Sigma M \Psi_{R} + h.c. \right)$$

$$- \frac{1}{4} W_{\mu\nu}^{a} W^{a\mu\nu} - \frac{1}{4} B_{\mu\nu} B^{\mu\nu} + \frac{v^{2}}{4} \operatorname{Tr} \left(D_{\mu} \Sigma^{\dagger} D^{\mu} \Sigma \right) , \qquad (68)$$

$$M = \begin{pmatrix} m_{t} & 0 \\ 0 & m_{b} \end{pmatrix} ,$$

$$D_{\mu}^{L} = \partial_{\mu} - i g \frac{\tau^{a}}{2} W_{\mu}^{a} - i g' \frac{Y}{2} B_{\mu} ,$$

$$D_{\mu}^{R} = \partial_{\mu} - i g' Q_{f} B_{\mu} .$$

Here, $Y = \frac{1}{3}$ is the hypercharge quantum number for the quark doublet, Q_f is the electric charge of the fermion, Ψ_L is the linearly realized left handed quark doublet, and Ψ_R is the right handed singlet for top or bottom quarks [cf. Eqs. (30) and (32)].

As we shall see shortly, in the context of this Lagrangian there is one (and only

one) diagram with the leading high energy power. Hence, we do not expect any cancellations among diagrams and it is possible to correctly predict the high energy behavior of the scattering amplitude. Here is how it works: When we expand the Σ matrix field up to the second power [cf. Eq. (1)] in the fermion mass term of Eq. (68), we will notice two things: (i) the first power term gives to the vertex ϕ^3 -t-t, and associates the coefficient $c_T = m_t/v$ to it; (ii) the second power term generates the four-point vertex [cf. Fig. 2(c)] with a coefficient $c_T = m_t^2/v^2$ associated to it. As it is well known, a $\overline{t}t = \overline{t}_R t_L + \overline{t}_L t_R$ term always involves a chirality flip, therefore we readily recognize that this four-point diagram will only participate when the chiralities of the top and anti-top are different. As $E \gg m_t$, different chiralities imply equal helicities for the fermion-antifermion pair. Hence, for the case of opposite helicities we only count the power dependance for diagrams 2(a) and 2(b), and take the highest one. For final state fermions of equal helicities we consider all three diagrams.

The results are the following: for diagrams 2(a) and 2(b) we have $D_{E0} = 2 + (-1) + (-1) = 0$, thus the amplitude $T_{\pm \mp}$ is of order m_t^2/v^2 (if there are no additional cancellations); which is the contribution given by the coefficients c_T from both vertices. On the other hand, diagram 2(c) has $D_{E0} = 2 - 1 = 1$; the equal helicities amplitude $T_{\pm \pm}$ will be driven by this dominant diagram, therefore $T_{\pm \pm} = m_t E/v^2$.

For the other processes; $W_L^+W_L^- \to t\bar{t}$ and $W_L^+Z_L \to t\bar{b}$, the analysis is the same, except that there is an extra s-channel diagram [cf. Figs. 4 and 5] whose high energy behavior is similar to the diagrams 2(a) and 2(b). Also, for the amplitude of $W_L^+Z_L \to t\bar{b}$ no four-point diagram 2(c) is generated; this means that its high energy behavior can at most be of order m_t^2/v^2 as given by diagrams 2(a) and 2(b).

In conclusion, in order to estimate the high energy behavior of the $V_L V_L \to t\bar{t}$, $t\bar{b}$ process, one has to write down the relevant diagrams for $\phi\phi\to t\bar{t}$, $t\bar{b}$ and then apply the power counting formula given in Eq. (67). If more than one diagram have the same leading power in E then one can suspect possible additional cancellations. This is the case for the dimension 4 non-linear chiral Lagrangian $\mathcal{L}_{SM}^{(4)}$ (Eq. (33) with κ 's equal to zero), for which all three diagrams 2(a), (b) and (c) grow as E^2 at high energies. Another gauge invariant Lagrangian for $\mathcal{L}_{SM}^{(4)} + \mathcal{L}^B$ is given in Eq. (68) which gives the same matrix elements for any physical process, but does not have the problem of possible cancellations among the Goldstone boson diagrams. With this Lagrangian the power counting formula predicts a leading E^1 behavior for $\phi^0\phi^0 \to t\bar{t}$ or $\phi^+\phi^- \to t\bar{t}$ (which originates from the four-point couplings that contributing to the diagram 2(c)), but only E^0 power for $\phi^\pm\phi^0 \to t\bar{b}$ or $b\bar{t}$ (which does not have the diagram similar to 2(c)). This is verified in Appendix B.

Notice that, in general, if the dimension 4 anomalous couplings κ 's are not zero, then there is no reason to expect any cancellations among the Goldstone boson diagrams. As a matter of fact, the calculated leading contributions from these coefficients are of order E^2 and not E^1 [cf. Appendix B].¹¹

¹¹This is related to the fact that non-zero anomalous κ terms break the linearly realized $SU(2)_L \times$

For the dimension 5 anomalous operators we do not suspect a priori any cancellations at high E among Goldstone boson diagrams, therefore we expect the parametrization used for our effective operators to reflect the correct high energy behavior. Actually, the chiral Lagrangian parametrization given by Eq. (34), which organizes the new physics effects in the momentum expansion, is the only framework that allows the existence of such dimension 5 gauge invariant operators. On the other hand, we know that as far as the no-Higgs SM contribution to these anomalous amplitudes is concerned, the correct high energy behavior is given by the equivalent parametrization of Eq. (68). We will therefore use the appropriate couplings from \mathcal{L}_{SM} and $\mathcal{L}^{(5)}$ in our next power counting analysis. Also, we are neglecting contributions of order $1/\Lambda^2$, which means that in diagrams 2(a) and 2(b) only one vertex is anomalous.

Given one dimension 5 operator, it either involves two boson fields (four-point operator), or one boson field and one derivative (three-point operator). Let us discuss four-point (4-pt) operators first.

There are three kinds of 4-pt operators: O_{ZZ} , O_{WW} and O_{WZ} . Each of them contributes to the $Z_L Z_L$, $W_L^+ W_L^-$ and $W_L^+ Z_L$ fusion processes separately. After expanding the composite boson fields Z and W^{\pm} [cf. Eqs. (19) and (20)], we find that the terms $\frac{4}{v^2} \partial_{\mu} \phi^3 \partial_{\nu} \phi^3$, $\frac{4}{v^2} \partial_{\mu} \phi^+ \partial_{\nu} \phi^-$ and $\frac{4}{v^2} \partial_{\mu} \phi^+ \partial_{\nu} \phi^3$ will contribute to a diagram of type 2(c) in each case. Therefore, in the power counting formula (67), $d_n = 2$, $c_T = 4a_O$ and $D_{E0} = 2 + (2 + 1 - 2) = 3$, which means that

$$T \sim 4a_O \frac{v}{\Lambda} \left(\frac{E}{v}\right)^3 \tag{69}$$

for all these 4-pt operators.

Let us discuss the case of 3-pt operators by considering one operator in particular: O_{ZDf} . This analysis will automatically apply to all the other six 3-pt; three with the neutral \mathcal{Z}_{μ} boson, O_{ZDf} , O_{gDZ} and $O_{\sigma DZ}$; and three with the charged \mathcal{W}_{μ} boson, O_{WDt} , O_{gDW} and $O_{\sigma DW}$. Using the expansions of the composite fields we obtain:

$$a_{z3}i\bar{t}\partial_{\mu}t\mathcal{Z}^{\mu} = -\frac{g}{c_{w}}a_{z3}i\overline{\psi}_{t}\partial_{\mu}\psi_{t}Z^{\mu} + \frac{2i}{v}a_{z3}\left[\overline{\psi}_{t}\partial_{\mu}\psi_{t}\partial^{\mu}\phi^{3}\right]$$

$$-\overline{\psi}_{t}\gamma_{5}\partial_{\mu}\psi_{t}\phi^{3}\partial^{\mu}\phi^{3} - \overline{\psi}_{tR}\partial_{\mu}\psi_{bL}\phi^{+}\partial^{\mu}\phi^{3} + \overline{\psi}_{t}\partial_{\mu}\psi_{t}(\phi^{-}\partial^{\mu}\phi^{+} - \phi^{+}\partial^{\mu}\phi^{-})\right] + \cdots$$

$$(70)$$

Where ψ_t (ψ_b) denotes the usual linearly realized top (bottom) quark field. There are more terms in Eq. (70) that participate in the Goldstone boson diagrams of interest, but the ones shown are sufficient for our discussion. Notice that the first two terms on the right hand side of Eq. (70) contribute to 3-pt vertices, the first one is for the coupling of the top quark with the usual vector boson field (the only non-zero

 $U(1)_Y$ gauge symmetry in the interaction part of Eq. (68). Notice that the κ terms respect this gauge symmetry only non-linearly.

term in the unitary gauge); the second one represents the vertex of O_{ZDf} that enters in diagrams 2(a) and 2(b) for $\phi^3\phi^3 \to t\bar{t}$, or in a *u-channel* diagram like 2(b) for $\phi^+\phi^3 \to t\bar{b}$. The rest of the expansion contains vertices with two or more boson fields. In Eq. (70), we also show some of the 4-pt vertices generated by O_{ZDf} , which dominate the contribution of this operator to the V_LV_L fusion processes in the high energy regime. The last term, $\bar{\psi}_t\partial_\mu\psi_t(\phi^-\partial^\mu\phi^+ - \phi^+\partial^\mu\phi^-)$, comes from the second order term in the expansion of \mathcal{Z}_μ [cf. Eq. (19)], and is responsible for the high energy behavior of the *s-channel* diagram for $W_L^+W_L^- \to t\bar{t}$ [cf. Fig. 4]. We can infer that the other two 3-pt operators with the \mathcal{Z}_μ field can also contribute to all the V_LV_L fusion processes. However, because of the relation $\epsilon_\mu p^\mu = 0$ for the on-shell external boson lines, the contributions of O_{gDZ} and $O_{\sigma DZ}$ vanish for $Z_LZ_L \to t\bar{t}$ and $W_LZ_L \to t\bar{b}$.

Notice that the expansion for W_{μ}^{\pm} in Eq. (20) does not contain any term with ϕ^3 alone; hence, no operator with the field W_{μ}^{\pm} can participate in the process $Z_L Z_L \to t \overline{t}$ at tree level. Except for this, the analysis on O_{ZDf} applies equally to the operators with W_{μ}^{\pm} . However, the contributions of O_{gDW} and $O_{\sigma DW}$ on the process $W_L^+ W_L^- \to t \overline{t}$ vanish because of the relation $\epsilon_{\mu} p^{\mu} = 0$ for the on-shell external boson lines.

The analysis on the high energy behavior of the contributions from O_{ZDf} to the scattering process $Z_L Z_L \to t\bar{t}$ is similar to the previous one for the no-Higgs SM, in which we observed a distinction between the $T_{\pm \mp}$ and $T_{\pm \pm}$ amplitudes. The anomalous vertices generated by this operator contain two derivatives, thus $(d_n + \frac{1}{2}f_n - 2) = 1$. Then, $D_{E0} = 2 + 1 + (-1) = 2$ for the first two diagrams 2(a) and 2(b), and $T_{\pm \mp}$ is of expected to be of order

$$T_{\pm\mp} \sim 2a_O \frac{m_t}{v} \frac{v}{\Lambda} \left(\frac{E}{v}\right)^2$$
.

On the other hand, diagram 2(c) comes from the first 4-pt term in Eq. (70). Thus, we have $(d_n + \frac{1}{2}f_n - 2) = 1$, $D_{E0} = 2 + 1 = 3$, and the predicted value for $T_{\pm\pm}$ is

$$T_{\pm\pm} \sim 2a_O \frac{v}{\Lambda} \left(\frac{E}{v}\right)^3$$
.

Comparing with the estimate for 4-pt operators [cf. Eq. (69)] we can observe that the only difference is in the coefficient c_T associated to them; for the three-point operator (70) $c_T = 2a_O$, and for a four-point operator is twice as much.¹²

Other possible contributions that vanish have to do with the fact that sometimes an amplitude can be zero from the product of two different helicities of spinors. For instance, by performing the calculation of the amplitudes in the CM frame we can easily verify that the spinor product $\overline{u}[\lambda = \pm 1]v[\lambda = \mp 1]$ vanishes for all $t\overline{t}$, $t\overline{b}$ and $b\overline{t}$ processes.¹³ This means that contributions from operators of the *scalar*-type, like

¹² This difference in c_T may be related to the fact that four-point operators tend to give a bigger contribution to the helicity amplitudes [cf. Eqs. (82) and (83), for example].

 $^{^{13}}u[\lambda=+1]$ denotes the spinor of a quark with right handed helicity.

 $O_{gWZL(R)}$, O_{gZZ} , O_{gWW} , O_{ZDf} , and $O_{WDtR(L)}$ will vanish for $T_{\pm\mp}$ amplitudes in the s-channel and the four-point diagrams.

Furthermore, the relation $\epsilon_{\mu}p^{\mu}=0$ applies to all the external on-shell boson lines; this makes the contribution of operators with derivative on boson, such as O_{gDZ} (our third case) and $O_{gDWL(R)}$, to vanish in the t- and u-channel diagrams. In principle, one would think that the exception could be the s-channel diagram. Actually, this is the case for the operator $O_{gDWL(R)}$ which contributes significantly to the single top production process $W_L^+Z_L \to t\bar{b}$ via the s-channel diagram [cf. Table 4]. However, for the O_{gDZ} operator even this diagram vanishes; as can be easily verified by noting that the Lorentz contraction between the boson propagator $-g_{\mu\nu} + k_{\mu}k_{\nu}/M_Z^2$ and the tri-boson coupling is identically zero in the process $W_L^+W_L^- \to t\bar{t}$. Therefore, for the O_{gDZ} operator all the possible diagrams vanish.

In Tables 2, 3, and 4 we show the leading contributions (in powers of the CM energy E) of all the operators for each different process; those cells with a dash mean that no anomalous vertex generated by that operator intervenes in the given process, and those cells with a zero mean that the anomalous vertex intervenes in the process but the amplitude vanishes for any of the reasons explained above.

Process	${\cal L}_{SM}^{(4)}$	O_{gZZ}	O_{gWW}	$O_{\sigma WW}$	$O_{gWZL(R)}$	$O_{\sigma W \mathcal{Z}L(R)}$
		$a_{zz1} \times$	$a_{ww1} \times$	$a_{ww2} \times$	$a_{wz1L(R)} \times$	$a_{wz2L(R)} \times$
$Z_L Z_L \to t \bar{t}$	$m_t E/v^2$	$E^3/v^2\Lambda$	_	_	_	_
$W_L^+W_L^- \to t\bar{t}$	$m_t E/v^2$	_	$E^3/v^2\Lambda$	$E^3/v^2\Lambda$	_	_
$W_L^+ Z_L \to t \overline{b}$	m_t^2/v^2	_	_	_	$E^3/v^2\Lambda$	$E^3/v^2\Lambda$

Table 2: The leading high energy terms for the 4-point operators.

Process	${\cal L}_{SM}^{(4)}$	$O_{\mathcal{Z}Df}$	$O_{\mathcal{W}DtR}$	$O_{\mathcal{W}DtL}$	
		$a_{z3} \times$	$a_{w3R} \times$	$a_{w3L} \times$	
$Z_L Z_L \to t \bar{t}$	$m_t E/v^2$	$E^3/v^2\Lambda$	_	_	
$W_L^+W_L^- \to t\bar{t}$	$m_t E/v^2$	$E^3/v^2\Lambda$	$E^3/v^2\Lambda$	$m_b E^2/v^2 \Lambda \to 0$	
$W_L^+ Z_L \to t \overline{b}$	m_t^2/v^2	$E^3/v^2\Lambda$	$E^3/v^2\Lambda$	$E^3/v^2\Lambda$	

Table 3: The leading high energy terms for the operators with derivative-on-fermion.

In conclusion, based on the NDA [25] and the power counting rule [31], we have found that the leading high energy behavior in the $V_L V_L \to t\bar{t}$ or $t\bar{b}$ scattering amplitudes from the no-Higgs SM operators $(\mathcal{L}_{SM}^{(4)})$ can only grow as $\frac{m_t E}{v^2}$ (for T_{++} or

Process	${\cal L}_{SM}^{(4)}$	$O_{gD\mathcal{Z}}$	$O_{gDWL(R)}$	$O_{\sigma D \mathcal{Z}}$	$O_{\sigma DWL(R)}$	$O_{\mathcal{A}}$
		$a_{z4} \times$	$a_{w4} \times$	$a_{z2} \times$	$a_{w2} \times$	$a_m \times$
$Z_L Z_L \to t \bar{t}$	$m_t E/v^2$	0	_	0	_	_
$W_L^+W_L^- \to t\bar{t}$	$m_t E/v^2$	0	0	$E^3/v^2\Lambda$	0	$E^3/v^2\Lambda$
$W_L^+ Z_L \to t \overline{b}$	m_t^2/v^2	0	$E^3/v^2\Lambda$	0	$E^3/v^2\Lambda$	_

Table 4: The leading high energy terms for the operators with derivative-on-boson.

 T_{--} ; E is the CM energy of the top quark system), whereas the contribution from the dimension 5 operators ($\mathcal{L}^{(5)}$) can grow as $\frac{E^3}{v^2\Lambda}$ in the high energy regime. Let us compare the above results with those of the $V_LV_L \to V_LV_L$ scattering processes. For these $V_LV_L \to V_LV_L$ amplitudes the leading behavior at the lowest order gives $\frac{E^2}{v^2}$, and the contribution from the next-to-leading order (NLO) bosonic operators gives $\frac{E^2}{\Lambda^2}\frac{E^2}{v^2}$ [31]. This indicates that the NLO contribution is down by a factor of $\frac{E^2}{\Lambda^2}$ in $V_LV_L \to V_LV_L$. On the other hand, the NLO fermionic contribution in $V_LV_L \to t\bar{t}$ or $t\bar{b}$ is only down by a factor $\frac{E^2}{m_t\Lambda}$ which compared to $\frac{E^2}{\Lambda^2}$ turns out to be bigger by a factor of $\frac{\Lambda}{m_t} \sim 4\sqrt{2}\pi$ for $\Lambda \sim 4\pi v^{14}$ Hence, we expect that the NLO contributions in the $V_LV_L \to t\bar{t}$ or $t\bar{b}$ processes can be better measured (by about a factor of 10) than the $V_LV_L \to V_LV_L$ counterparts for some class of electroweak symmetry breaking models in which the NDA gives reasonable estimates of the coefficients.

As will be shown later, the coefficients of the NLO fermionic operators in $\mathcal{L}^{(5)}$ can be determined via top quark production to an order of 10^{-2} or 10^{-1} . In contrast, the coefficients of the NLO bosonic operators are usually determined to about an order of 10^{-1} or 1 [21, 24] via $V_L V_L \to V_L V_L$ processes. Therefore, we conclude that the top quark production via longitudinal gauge boson fusion $V_L V_L \to t\bar{t}, t\bar{b}$, or $b\bar{t}$ at high energy may be a better probe, for some classes of symmetry breaking mechanisms, than the scattering of longitudinal gauge bosons, i.e. $V_L V_L \to V_L V_L$.

In the following section we shall study the production rates of $t\bar{t}$ pairs and single-t or single- \bar{t} events at future colliders like LHC and LC. We will also estimate how precisely these NLO fermionic operators can be measured via the $V_L V_L \to t\bar{t}, t\bar{b}$, or $b\bar{t}$ processes. To reduce the number of independent parameters for our discussion, we shall assume an approximate custodial SU(2) symmetry, so that the set of 19 independent coefficients will be reduced to 6 and given by $a_{zz1}, a_{z2}, a_{z3}, a_{z4}, a_{ww2}$, and a_m . However, for completeness we also give the leading high energy contributions of the helicity amplitudes for $Z_L Z_L \to t\bar{t}, W_L^- W_L^+ \to t\bar{t}, W_L^+ Z_L \to t\bar{b}$ and $W_L^- Z_L \to b\bar{t}$ in Appendices B and C.

The For an energy E of about $\Lambda/4$ or more this factor $\frac{E^2}{m_t\Lambda} = \frac{M^{(5)}}{M^{(4)}}$ is actually greater than one. $M^{(4)}$ and $M^{(5)}$ are the LO and NLO amplitudes, respectively.

6 Underlying custodial symmetry

Here, we shall consider a special class of models of symmetry breaking for which an approximate underlying custodial symmetry [32] is assumed as suggested by the low energy data [4].

In addition to the gauge symmetry, the SM has an approximate global symmetry called the custodial symmetry which is responsible for the tree-level relation $\rho \simeq 1$ [cf. Eq. (4)]. Actually, this symmetry is broken by the hypercharge (g') and the mass splitting $(m_t \neq m_b)$, but only slightly, so that ρ remains about one at the one loop level. After turning off the hypercharge coupling (i.e. set $s_w = 0$), one can easily verify that the global $SU(2)_L \times SU(2)_R$ symmetry is satisfied for the dimension 4 Lagrangian $\mathcal{L}_{SM}^{(4)}$. The fermion-gauge boson interactions are described by

$$\mathcal{L}^{(4custodial)} = \overline{F_L} \gamma^{\mu} \left(i \partial_{\mu} - \frac{1}{2} \mathcal{W}_{\mu}^{a} \tau^{a} \right) F_L , \qquad (71)$$

with the left handed doublet

$$F_L = \begin{pmatrix} f_1 \\ f_2 \end{pmatrix}_L \tag{72}$$

defined in Eq. (30).

Notice that the only SU(2) structure that satisfies the custodial symmetry is the one given above. If we want to introduce an anomalous interaction that satisfies this symmetry, we must conform to this structure. For example, let us consider the case of the operators with derivative on boson O_{gDZ} and $O_{gDWL(R)}$, then we write:¹⁶

$$\kappa \overline{F_L} g^{\mu\nu} \partial_{\mu} \mathcal{W}_{\nu}^a \tau^a F_R + h.c. = \kappa \overline{F_L} g^{\mu\nu} \left(\begin{array}{cc} \partial_{\mu} \mathcal{W}_{\nu}^3 & \sqrt{2} \partial_{\mu} \mathcal{W}_{\nu}^+ \\ \sqrt{2} \partial_{\mu} \mathcal{W}_{\nu}^- & -\partial_{\mu} \mathcal{W}_{\nu}^3 \end{array} \right) F_R + h.c. . \quad (73)$$

As we can see, if we want our dimension 5 terms to obey this global $SU(2)_L \times SU(2)_R$ symmetry, we have to introduce the same anomalous interactions of the top quark to the much lighter bottom quark. Let us consider the case of an underlying global $SU(2)_L \times SU(2)_R$ symmetry that is broken in such a way as to account for a negligible deviation of the b-b-Z vertex from its standard form. Since the top quark acquires a mass much heavier than the other quarks' masses, we expect the new physics effects associated with the electroweak symmetry breaking (EWSB) sector to be substantially greater for the couplings (to the gauge bosons) of this quark than for the couplings of all the others (including the bottom quark). Therefore, it is probable that the underlying theory of particle physics respects the custodial symmetry, and the EWSB mechanism introduces an effective interaction that explicitly breaks this

To verify this, we just need to use the transformation rules $\Sigma \to \Sigma' = L\Sigma R^{\dagger}$ and $F_L \to F_L' = RF_L$, where L and R are group elements of the global $SU(2)_L$ and $SU(2)_R$ symmetries, respectively.

16 For the purpose of this discussion we can replace D_{μ} by ∂_{μ} .

symmetry in such a way as to favor the deviation of the couplings of the top quark more than the deviation of the other light quarks' couplings.

By adding the two possible breaking terms to this operator, ¹⁷ we obtain the effective dimension 5 Lagrangian as:

$$\mathcal{L}^{(5deriv)} = \kappa \overline{F_L} g^{\mu\nu} \partial_{\mu} \mathcal{W}^a_{\nu} \tau^a F_R + \kappa_1 \overline{F_L} g^{\mu\nu} \tau^3 \partial_{\mu} \mathcal{W}^a_{\nu} \tau^a F_R + \kappa_2 \overline{F_L} g^{\mu\nu} \partial_{\mu} \mathcal{W}^a_{\nu} \tau^a \tau^3 F_R + h.c. \qquad (74)$$

$$= \overline{F_L} g^{\mu\nu} \left(\frac{(\kappa + \kappa_1 + \kappa_2) \partial_{\mu} \mathcal{W}^3_{\nu}}{\sqrt{2}(\kappa + \kappa_1 - \kappa_2) \partial_{\mu} \mathcal{W}^+_{\nu}} \sqrt{2}(\kappa + \kappa_1 - \kappa_2) \partial_{\mu} \mathcal{W}^+_{\nu}} \right) F_R + h.c. ,$$

where, in order to obtain a vanishing b-b-Z coupling, we require

$$\kappa = \kappa_1 + \kappa_2. \tag{75}$$

Also, to simplify the discussion we assume $\kappa_1 = \kappa_2$, and the conclusion is that in order to keep the couplings b-b-Z unaltered we have to impose the condition

$$a_{z(2,3,4)} = \sqrt{2}a_{w(2,3,4)L(R)} \tag{76}$$

to all the operators with derivatives.

The case for 4-point operators (contact terms) is somewhat different. The custodial Lagrangian in this case is of the form:

$$\mathcal{L}^{(5custod)} = \kappa_{1g}^{4pt.} \overline{F_L} g^{\mu\nu} \mathcal{W}_{\mu}^a \tau^a \mathcal{W}_{\nu}^b \tau^b F_R + \kappa_{1\sigma}^{4pt.} \overline{F_L} \sigma^{\mu\nu} \mathcal{W}_{\mu}^a \tau^a \mathcal{W}_{\nu}^b \tau^b F_R$$

$$= \kappa_{1g}^{4pt.} \overline{F_L} \begin{pmatrix} \mathcal{W}_{\mu}^3 \mathcal{W}^{\mu 3} + 2\mathcal{W}_{\mu}^+ \mathcal{W}^{\mu -} & 0 \\ 0 & \mathcal{W}_{\mu}^3 \mathcal{W}^{\mu 3} + 2\mathcal{W}_{\mu}^+ \mathcal{W}^{\mu -} \end{pmatrix} F_R$$

$$+ \kappa_{1\sigma}^{4pt.} \overline{F_L} \sigma^{\mu\nu} \begin{pmatrix} 2\sigma^{\mu\nu} \mathcal{W}_{\mu}^+ \mathcal{W}_{\nu}^- & 0 \\ 0 & 2\sigma^{\mu\nu} \mathcal{W}_{\mu}^+ \mathcal{W}_{\nu}^- \end{pmatrix} F_R, \qquad (77)$$

and for the breaking terms we can consider:

$$\mathcal{L}^{(5contact)} = \sum_{c=g,\sigma} c^{\mu\nu} \left(\kappa_{2c}^{4pt.} \overline{F_R} \tau^3 \mathcal{W}_{\mu}^a \tau^a \mathcal{W}_{\nu}^b \tau^b F_L + \kappa_{2c}^{4pt.\dagger} \overline{F_L} \mathcal{W}_{\mu}^a \tau^a \mathcal{W}_{\nu}^b \tau^b \tau^3 F_R + \kappa_{3c}^{4pt.} \overline{F} \mathcal{W}_{\mu}^a \tau^a \tau^3 \mathcal{W}_{\nu}^b \tau^b F \right) ,$$

$$(78)$$

where κ_{2c}^{4pt} is complex and κ_{3c}^{4pt} is real. As it turns out, in order to set the anomalous couplings of the bottom quark equal to zero, we have to choose $\kappa_{3c}^{4pt} = 0$, and κ_{2c}^{4pt} real and half the size of κ_{1c}^{4pt} (i.e. $\kappa_{1c}^{4pt} = 2\kappa_{2c}^{4pt}$ for $c = g, \sigma$). The non-standard 4-point dimension 5 interactions will then have the structure

$$\begin{pmatrix}
c^{\mu\nu}W_{\mu}^{3}W_{\nu}^{3} + 2c^{\mu\nu}W_{\mu}^{+}W_{\nu}^{-} & 0\\
0 & 0
\end{pmatrix}$$
(79)

¹⁷ Another term could be $\overline{F_L}g^{\mu\nu}\tau^3\partial_{\mu}W^a_{\nu}\tau^a\tau^3F_R$, which contains two symmetry breaking factors τ^3 and will not be considered in this work.

where $c^{\mu\nu}$ is either $g^{\mu\nu}$ or $\sigma^{\mu\nu}$. This structure suggests $2a_{zz1}=a_{ww1}$, and $a_{wz1L(R)}=a_{wz2L(R)}=0$ for $c^{\mu\nu}$ equal to $g^{\mu\nu}$. For $c^{\mu\nu}$ equal to $\sigma^{\mu\nu}$, it suggests that a_{ww2} can be of any value.

In conclusion, by assuming the dimension 5 operators are the result of an underlying custodial symmetric theory that is broken in such a way that at tree level the Z-b-b coupling does not get modified from its SM values, we derive the following relations among the coefficients of these anomalous couplings. They are:

$$a_{z(2,3,4)} = \sqrt{2}a_{w(2,3,4)L(R)} ,$$

 $2a_{zz1} = a_{ww1} ,$ (80)
 $a_{wz1L(R)} = a_{wz2L(R)} = 0 .$

After including the hypercharge interactions, we can see that the set of independent coefficients has reduced from a total of 19 down to 6 only. These coefficients are $a_{z(2,3,4)}$, a_{zz1} , a_{ww2} and a_m (for the operator O_A).

7 Amplitudes for Z_LZ_L , W_LW_L , and W_LZ_L fusion processes

Below, we present the helicity amplitudes for each $V_L V_L$ fusion process. We shall only consider the leading contributions in powers of E, the CM energy of the $V_L V_L$ system, coming from both the no-Higgs SM (i.e. $\mathcal{L}_{SM}^{(4)}$) and the dimension 5 operators. For the latter, we assume an approximate SU(2) custodial symmetry, as discussed in the previous section, so that only 6 independent coefficients are relevant to our discussion. For completeness, in Appendices B and C we provide the helicity amplitudes for the general case (without assuming a custodial symmetry).

7.1 $Z_L Z_L \rightarrow t \bar{t}$

Fig. 3 shows the diagrams associated to this process. The total amplitude T is the sum of the $\mathcal{L}_{SM}^{(4)}$ contribution (denoted by zz), and the $\mathcal{L}^{(5)}$ contribution (denoted by azz). In diagrams with two vertices, only one anomalous vertex is considered at a time, i.e. we neglect contributions suppressed by $1/\Lambda^2$. We denote the helicity amplitudes by the helicities of the outgoing fermions: the first (second) symbol (+ or -) refers to the fermion on top (bottom) part of the diagram. A right handed fermion is labelled by '+', and a left handed fermion by '-'. For instance,

$$T_{zz++} = zz_{++} + azz_{++} , (81)$$

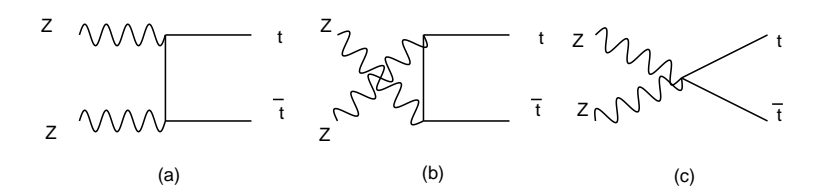


Figure 3: Diagrams for the $ZZ \to t\bar{t}$ process.

where zz_{++} is the $\mathcal{L}_{SM}^{(4)}$ contribution, and azz_{++} is the anomalous contribution to the helicity amplitude $T(Z_LZ_L \to t_{Right-handed}\bar{t}_{Right-handed})$. The same notation is used for the other two processes.

The leading contributions to the $Z_L Z_L \to t\bar{t}$ helicity amplitudes are:

$$T_{zz++} = -T_{zz--} = \frac{m_t E}{v^2} - \frac{2E^3 X}{v^2 \Lambda},$$

$$T_{zz+-} = T_{zz-+} = \frac{2 m_t^2 c_\theta s_\theta}{\left(\frac{4c_\theta^2 m_t^2}{E^2} + s_\theta^2\right) v^2} + 0,$$
(82)

where

$$X = a_{zz1} + \left(\frac{1}{2} - \frac{4}{3}s_w^2\right)a_{z3} , \qquad (83)$$

and $E = \sqrt{s}$ is the CM energy of the $V_L V_L$ system.

Comparing with the results for $W_L^+W_L^-$ and $W_L^+Z_L$ fusions, this is the amplitude that takes the simplest form with no angular dependance. Also, for this process the assumption of an underlying custodial symmetry does not make the anomalous contribution any different from the most general expression given in Appendix C. This means that new physics effects coming through this process can only modify the Spartial wave amplitude (at the leading order of E^3). Notice that at this point it is impossible to distinguish the effect of the coefficient a_{zz1} from the effect of the coefficient a_{z3} . However, in the next section we will show how to combine this information with the results of the other processes, and obtain bounds for each coefficient. The reason why $azz_{\pm\mp}$ appear as zero is explained in Appendix C.

7.2 $W_L^+W_L^- \to t\bar{t}$

The amplitudes of this process are similar to the ones of the previous process except for the presence of two s-channel diagrams (see Fig. 4), whose off-shell γ and Z propagators allow for the additional contribution from the magnetic moment of the top quark (a_m) and the operator with derivative on boson $O_{\sigma DZ}$ (a_{zz}) . Since these two operators are not of the scalar-type, we have a non-zero contribution to the $T_{\pm \mp}$ amplitudes. Throughout this paper, the angle of scattering θ in all processes is defined to be the one subtended between the incoming gauge boson that appears on

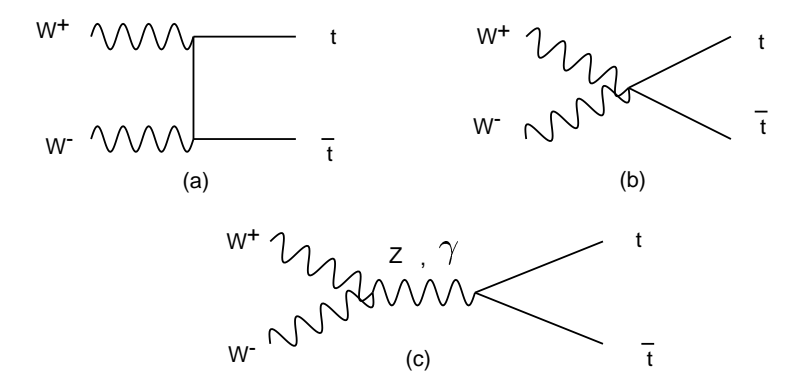


Figure 4: Diagrams for the $WW \to t\bar{t}$ process.

the top-left part of the Feynman diagram (W^+ in this case) and the momentum of the outgoing fermion appearing on the top-right part of the same diagram (t in this case); all in the CM frame of the V_LV_L pair.

The leading contributions to the various helicity amplitudes for this process are:

$$T_{ww++} = -T_{ww--} = \frac{m_t E}{v^2} - \frac{4 E^3}{v^2} \frac{(X_1 + X_m c_\theta)}{\Lambda} ,$$

$$T_{ww+-} = \frac{2 m_t^2 s_\theta}{\left(\frac{2m_b^2}{E^2} + (1 - c_\theta) \left(1 - \frac{2m_t^2}{E^2}\right)\right) v^2} + \frac{8E^2}{v^2} m_t s_\theta \frac{\left(X_m - \frac{1}{4} a_{z3}\right)}{\Lambda} ,$$

$$T_{ww-+} = 0 + \frac{8E^2}{v^2} m_t s_\theta \frac{X_m - \frac{1}{8} a_{z3}}{\Lambda} ,$$
(84)

where $s_{\theta} = \sin \theta$, $c_{\theta} = \cos \theta$, and

$$X_{1} = a_{zz1} + \frac{1}{8}a_{z3} ,$$

$$X_{m} = a_{m} - \frac{1}{2}a_{z2} + \frac{1}{8}a_{z3} + \frac{1}{2}a_{ww2} .$$
(85)

Notice that the angular distribution of the leading contributions in the $T_{\pm\pm}$ amplitudes consists of the flat component (S-wave) and the $d_{0,0}^1 = \cos\theta$ component (P-wave). The $T_{\pm\mp}$ helicity amplitudes only contain the $d_{0,\pm 1}^1 = -\frac{\sin\theta}{\sqrt{2}}$ component. This is so because the initial state consists of longitudinal gauge bosons and has zero helicity. The final state is a fermion pair so that the helicity of this state can be -1, 0, or +1. Therefore, in high energy scatterings, the anomalous dimension 5 operators only modify (at the leading orders E^3 and E^2) the S- and P-partial waves of the scattering amplitudes. We also note that, as expected from the discussion in section 5, $aww_{\pm\pm}$ has an E^3 leading behavior, whereas $aww_{\pm\mp}$ goes like E^2 . Furthermore, the $\mathcal{L}_{SM}^{(4)}$ amplitudes are of order $m_t E/v^2$ for $ww_{\pm\pm}$, and m_t^2/v^2 for ww_{+-} . (ww_{-+} is proportional to m_b^2/v^2 and is taken as

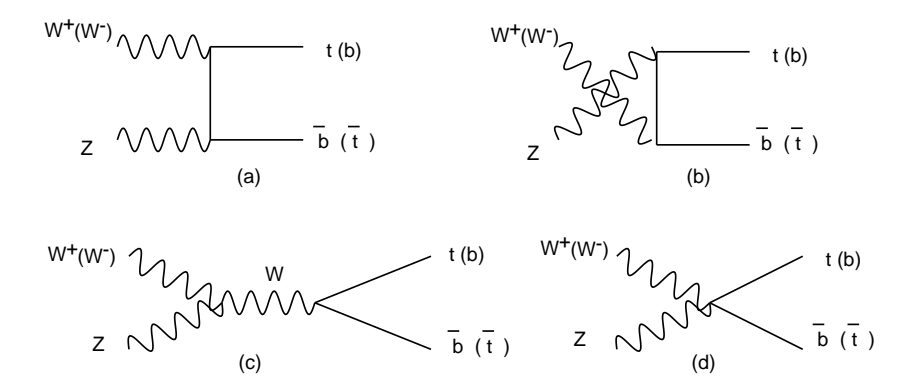


Figure 5: Diagrams for the $WZ \to t\bar{b}$ process.

zero.) To calculate the event rate, we need to sum over four helicity amplitudes squared, and $|T_{\pm\pm,\pm\mp}|^2 = ww_{\pm\pm,\pm\mp}^2 + 2ww_{\pm\pm,\pm\mp} aww_{\pm\pm,\pm\mp} + O(1/\Lambda^2)$. Because $|ww_{\pm\mp} aww_{\pm\mp}| \sim \frac{m_t^2}{E^2} |ww_{\pm\pm} aww_{\pm\pm}|$, the amplitude squared $|T_{\pm\mp}|^2$ is only a few percent of the value of $|T_{\pm\pm}|^2$ for $E \sim 1$ TeV. Thus, $|T_{\pm\mp}|^2$ will not contribute largely to the total event rate, provided the coefficients of the dimension 5 operators are of order one.

7.3 $W_L^+ Z_L \to t\bar{b}$

Finally, we have the amplitudes for the single-top quark production process $W^+Z \to t\bar{b}$ (which are just the same as for the conjugate process $W^-Z \to b\bar{t}$). Fig. 5 shows the diagrams that participate in this process.

The leading contributions to the various helicity amplitudes for this are:¹⁸

$$T_{wzt++} = -\frac{\sqrt{2} m_t^3 (1 - c_\theta)}{E \left(1 - \frac{2m_t^2}{E^2}\right) \left(1 + c_\theta + \frac{2m_t^2}{E^2}\right) v^2} - \frac{\sqrt{2}E^3}{4v^2} \frac{(X_2 + c_\theta X_3)}{\Lambda} ,$$

$$T_{wzt--} = 0 - \frac{\sqrt{2}E^3}{4v^2} \frac{\left((4s_w^2 a_{z4} + \frac{2}{3}s_w^2 - 1) + (a_{z3} - 4c_w^2 a_{z2})c_\theta\right)}{\Lambda} ,$$

$$T_{wzt+-} = 0 + \frac{\sqrt{2}E^2}{4v^2} m_t s_\theta \frac{(a_{z3} + 4c_w^2 a_{z2})}{\Lambda} ,$$

$$T_{wzt-+} = -\frac{\sqrt{2} m_t^2 s_\theta}{\left(1 - \frac{2m_t^2}{E^2}\right) \left(1 + c_\theta + \frac{2m_t^2}{E^2}\right) v^2} - \frac{3\sqrt{2}E^2}{4v^2} m_t s_\theta \frac{X_4}{\Lambda} ,$$
(86)

where

$$X_2 = \left(1 + \frac{2}{3}s_w^2\right)a_{z3} - 4s_w^2a_{z4} ,$$

¹⁸As shown in Eq. (80), for models with this approximate custodial symmetry, $a_{wz1L(R)} = a_{wz2L(R)} = 0$, so that the 4-point vertex diagram of Fig. 5(d) gives no contribution.

$$X_{3} = a_{z3} + 4c_{w}^{2}a_{z2} ,$$

$$X_{4} = a_{z3} - \frac{4}{3}c_{w}^{2}a_{z2} .$$
(87)

The anomalous amplitudes $awzt_{--}$ and $awzt_{+-}$ can be ignored in our analysis. The reason is because the $\mathcal{L}^{(4)}$ amplitudes wzt_{--} and wzt_{+-} are zero, which means that, when we consider the total helicity amplitudes squared, they turn out to be of order $1/\Lambda^2$. This is why only $awzt_{++}$ and $awzt_{-+}$ are presented in terms of the parameters X_2 , X_3 and X_4 , each parameter associated to a different partial wave.

8 Numerical Results

8.1 Top quark production rates from V_LV_L fusions

As discussed above, the top quark productions from $V_L V_L$ fusion processes can be more sensitive to the electroweak symmetry breaking sector than the longitudinal gauge boson productions from $V_L V_L$ fusions. In this section we shall examine the possible increase (or decrease) of the top quark event rates, due to the anomalous dimension 5 couplings, at the future hadron collider LHC (a pp collider with $\sqrt{s} = 14$ TeV and 100 fb⁻¹ of integrated luminosity) and the electron linear collider LC (an e^-e^+ collider with $\sqrt{s} = 1.5$ TeV and 200 fb⁻¹ of integrated luminosity).

To simplify our discussion, we shall assume an approximate custodial symmetry and make use of the helicity amplitudes given in the previous section to compute the production rates for $t\bar{t}$ pairs and for single-t or \bar{t} quarks. We shall adopt the effective-W approximation method [9, 33], and use the CTEQ3L [34] parton distribution function with the factorization scale chosen to be the mass of the W-boson. For this study we do not intend to do a detailed Monte Carlo simulation for the detection of the top quark; therefore, we shall only impose a minimal set of cuts on the produced t or b. The rapidity of t or b produced from the V_LV_L fusion process is required to be within 2 (i.e. $|y^{t,b}| \leq 2$) and the transverse momentum of t or b is required to be at least 20 GeV. To validate the effective-W approximation, we also require the invariant mass M_{VV} to be larger than 500 GeV.

Since we are working in the high energy regime $E \gg v$, the approximation made when we expand the $V_L V_L \to t\bar{t}$ or $t\bar{b}$ scattering amplitudes in powers of E and keep the leading terms only, becomes a very good one. As noted in the previous section, in all the $T_{\pm\pm}$ amplitudes, the dimension 5 operators will only modify the constant term (S-wave) and the $\cos\theta$ (P-wave: $d_{0,0}^1$) dependence in the angular distributions of the leading E^3 contributions, whereas all the $T_{\pm\mp}$ amplitudes have a $\sin\theta$ (P-wave: $d_{0,\pm 1}^1$) dependence in their leading E^2 contributions. Each of the effective coefficients, X,

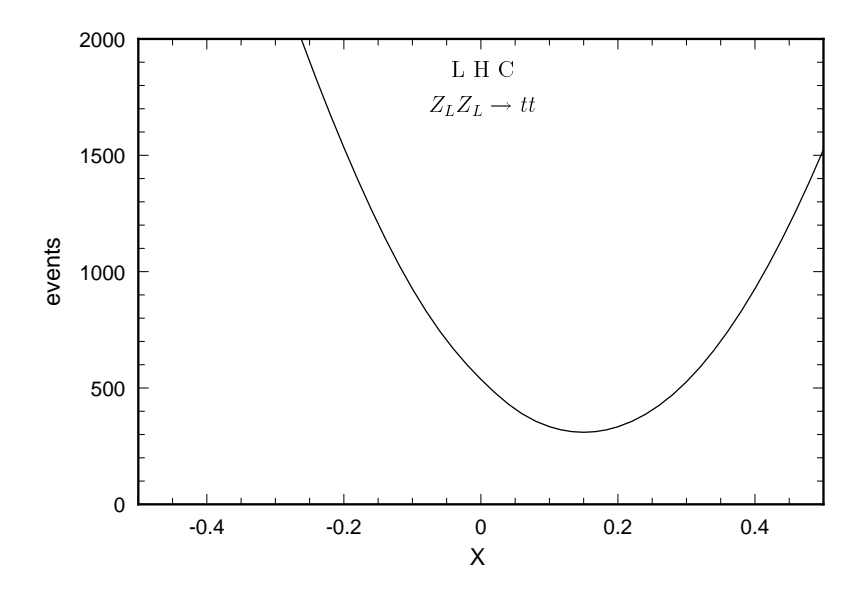


Figure 6: Number of events at the LHC for $Z_L Z_L$ fusion. The variable X is defined in Eq. (83).

 X_1 , X_m , X_2 , X_3 and X_4 , parametrizes the contribution to one of the partial waves.¹⁹ Since contributions to different partial waves do not interfere with each other, we can make a consistent analysis by taking only one coefficient non-zero at a time.

The predicted top quark event rates as a function of these coefficients are given in Figs. 6, 7 and 8 for the LHC, and in Figs. 9, 10 and 11 for the LC. In these plots, neither the branching ratio nor the detection efficiency have been included.

For X=0, the LHC results show that there are in total about 1500 $t\bar{t}$ pair and single-t or \bar{t} events predicted by the no-Higgs SM. The $W_L^+W_L^-$ fusion rate is about a factor of 2 larger than the Z_LZ_L fusion rate, and about an order of magnitude larger than the $W_L^+Z_L$ fusion rate. The $W_L^-Z_L$ rate, which is not shown here, is about a factor of 3 smaller than the $W_L^+Z_L$ rate due to smaller parton luminosities at a pp collider. It will be challenging to actually detect any signal from these channels at the LHC due to the considerable amount of background in this hadron-hadron collision. What we can learn from Fig. 7 is that, with a production of about 900 events and the large slope of the $W_L^+W_L^- \to t\bar{t}$ curve, this process might be able to probe the anomalous coupling (X_1) .

For the LC, because of the small coupling of Z-e-e, the event rate for $Z_L Z_L \to t \overline{t}$ is small. For the no-Higgs SM, the top quark event rate at LC is about half of that at the LHC and yields a total of about 550 events ($t \overline{t}$ pairs and single-t or \overline{t}). Again, we find that the $W_L^+ W_L^- \to t \overline{t}$ rate is sensitive to the dimension 5 operators that

¹⁹In $W_L^+W_L^- \to t\overline{t}$, X_m contributes to both P-partial waves.

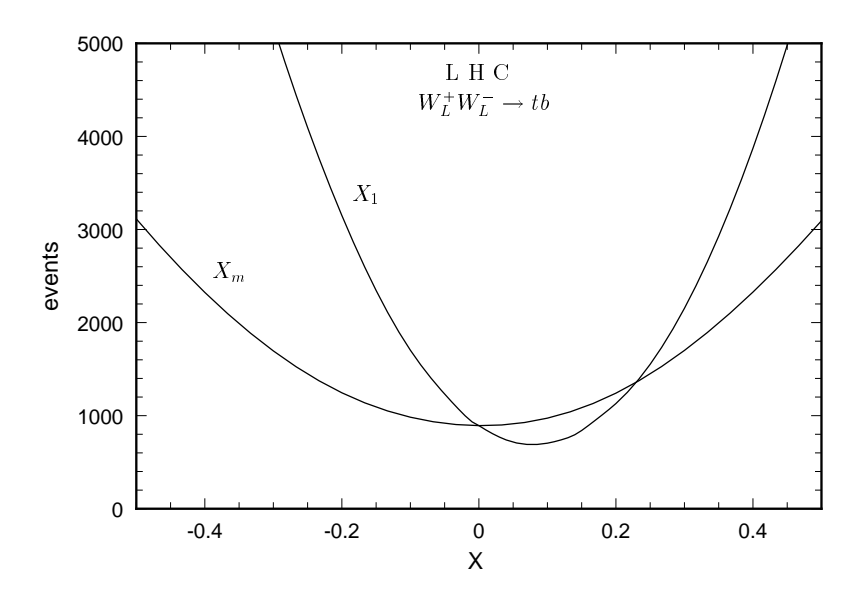


Figure 7: Number of events at the LHC for $W_L^+W_L^-$ fusion. The variable X stands for the effective coefficients X_1 and X_m defined in Eq. (85).

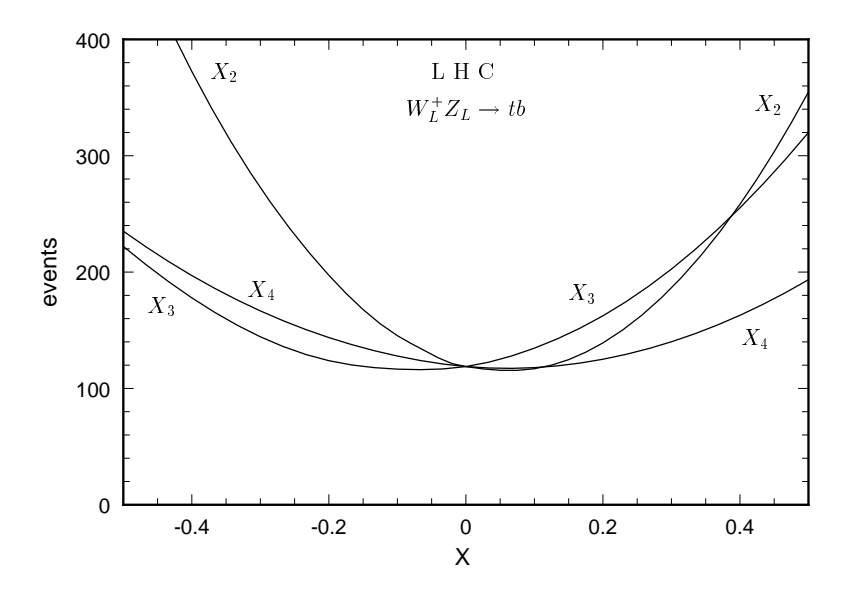


Figure 8: Number of events at the LHC for $W_L^+ Z_L$ fusion. The variable X stands for the effective coefficients X_2 , X_3 and X_4 defined in Eq. (87).

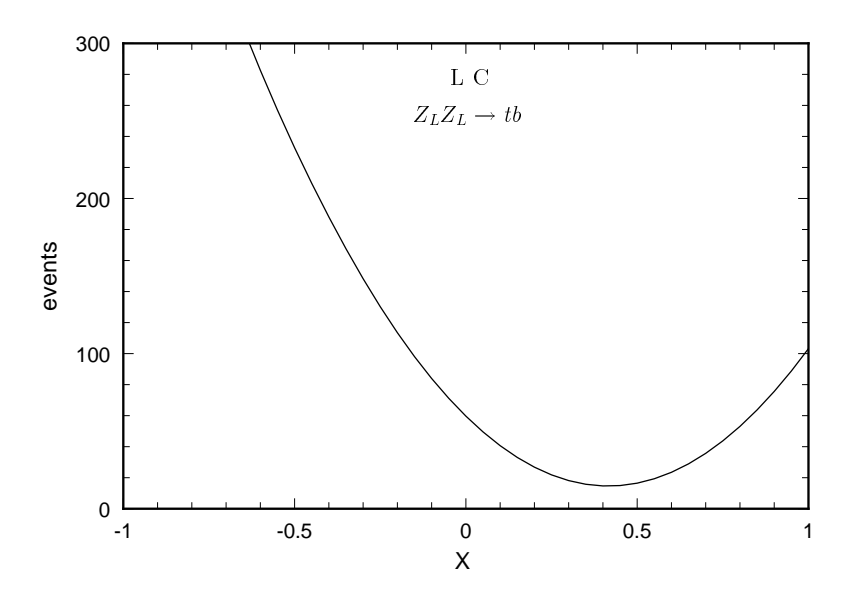


Figure 9: Number of events at the LC for $Z_L Z_L$ fusion. The variable X is defined in Eq. (83).

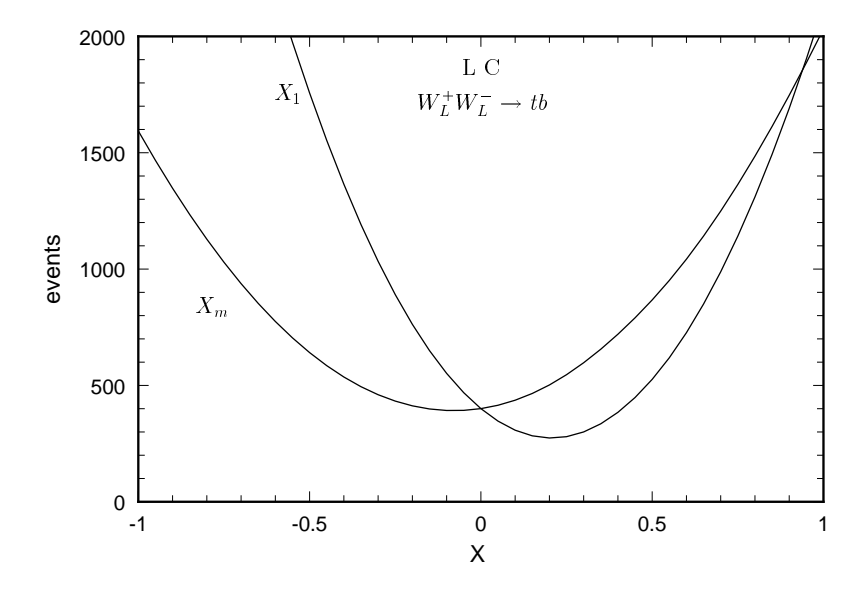


Figure 10: Number of events at the LC for $W_L^+W_L^-$ fusion. The variable X stands for the effective coefficients X_1 and X_m defined in Eq. (85).

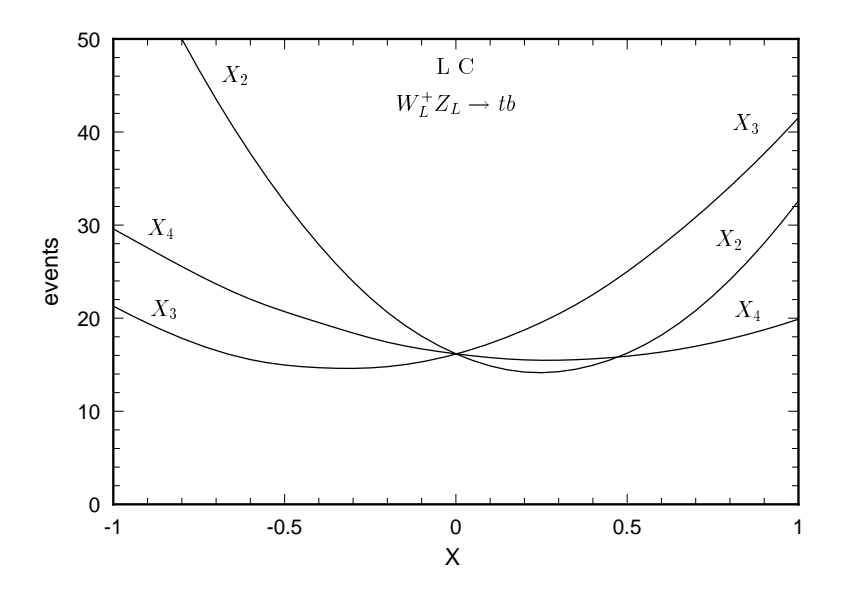


Figure 11: Number of events at the LC for $W_L^+ Z_L$ fusion. The variable X stands for the effective coefficients X_2 , X_3 and X_4 defined in Eq. (87).

correspond to X_1 , but the $Z_L Z_L \to t\bar{t}$ rate is much less sensitive.²⁰

The production rates shown in Figs. 9, 10 and 11 are for an unpolarized e^- beam at the LC. Because the coupling of the W boson to the electron is purely left handed, the parton luminosity of the W boson will double for a left-handed polarized e^- beam at the LC; hence, the $t\bar{t}$ rate from $W_L^+W_L^-$ fusion will double too. However, this is not true for the parton luminosity of Z because in this case the Z-e-e coupling is nearly purely axial-vector $(1-4s_w^2\approx 0)$ and the production rate of $Z_LZ_L\to t\bar{t}$ does not strongly depend on whether the electron beam is polarized or not. As shown in these plots, if the anomalous dimension 5 operators can be of order 10^{-1} (as expected by the naive dimensional analysis) then their effect can in principle be identified in the measurement of either Z_LZ_L or $W_L^+W_L^-$ fusion rates at the LC. ²¹ A similar conclusion holds for the $W_L^\pm Z_L$ fusion process, but with less sensitivity.

From the six independent coefficients, $a_{z(2,3,4)}$, a_{zz1} , a_{ww2} and a_m , one stands out: a_{zz1} . The two most potentially significant parameters X and X_1 depend essentially on just this coefficient [cf. Eqs. (83) and (85)]. This suggests that a good test for the possible models of EWSB is to calculate their predictions for the sizes of the four point operators O_{gZZ} and O_{gWW} because these are more likely to produce a measurable signal at either the LC or the LHC. The second better test could be the magnetic moment a_m because this coefficient gives the largest contribution to X_m [cf. Eq. (85)], and Figs. 7 and 10 show that this parameter can be measured as well.

 $^{^{20}}$ Needless to say, the $W_L^- Z_L$ rate is the same as the $W_L^+ Z_L$ rate at an unpolarized $e^+ e^-$ LC

²¹ Specifically, for anomalous coefficients of order 10^{-1} there is a 2σ deviation from the *no-Higgs* SM event rates.

It is useful to ask for the bounds on the coefficients of the anomalous dimension 5 operators if the measured production rate at the LC is found to be in agreement with the no-Higgs SM predictions (i.e. with X=0). In order to simplify this analysis for the parameter X_m , we have made the approximation $aww_{+-} \simeq \frac{8E^2}{v^2} m_t s_\theta \frac{X_m}{\Lambda}$; notice that the anomalous contribution aww_{+-} to the total amplitude squared is smaller by a factor of m_t^2/E^2 than the contribution from $aww_{\pm\pm}$ [cf. end of section 7.2].

At the 95% C.L. we summarize the bounds on the X's in Table 5. Here, only the statistical error is included. In practice, after including the branching ratios of the relevant decay modes and the detection efficiency of the events, these bounds will become somewhat weaker, but we do not expect an order of magnitude difference. Also, these bounds shall be improved by carefully analyzing angular correlations when data is available.

Process	Bounds (e^+e^-)
$Z_L Z_L \to t \bar{t}$	-0.07 < X < 0.08
$W_L^+W_L^- \to t\bar{t}$	$-0.03 < X_1 < 0.035$
$W_L^+W_L^- \to t\bar{t}$	$-0.28 < X_m < 0.12$
$W_L^{+(-)}Z_L \to t\bar{b}\ (b\bar{t})$	$-0.32 < X_2 < 0.82$
$W_L^{+(-)}Z_L \to t\bar{b}\ (b\bar{t})$	$-1.2 < X_3 < 0.5$
$W_L^{+(-)}Z_L \to t\bar{b}\ (b\bar{t})$	$-0.8 < X_4 < 1.3$

Table 5: The range of parameters for which the total number of events at the LC deviates by less than 2σ from the *no-Higgs* SM prediction.

As shown in Table 5, these coefficients can be probed to about an order of 10^{-1} or even 10^{-2} . For this Table, we have only considered an unpolarized e^- beam for the LC. To obtain the bounds we have set all the anomalous coefficients to be zero except the one of interest. This procedure is justified by the fact that at the leading orders of E^3 and E^2 , different coefficients contribute to different partial waves. (The definitions of the combined coefficients X, X_1 , X_2 , X_3 and X_4 are given in the previous section.)

If the LC is operated at the e^-e^- mode with the same CM energy of the collider, then it cannot be used to probe the effects for $W_L^+W_L^- \to t\bar{t}$, but it can improve the bounds on the combined coefficients X_4 , X_2 and X_3 , because the event rate will increase by a factor of 2 for $W_L^-Z_L \to b\bar{t}$ production.

By combining the limits on these parameters we can find the corresponding limits on the effective coefficients a_{zz1} , a_{z2} , a_{z3} , a_{z4} , and $(a_m + \frac{1}{2}a_{ww2})$. For example, if we consider the limits for X_3 and X_4 , we will find the limits for a_{z2} , a_{z3} . Then we can compare the bounds on a_{z3} and those on X_1 to derive the constraints on a_{zz1} . Also, the bounds on a_{z3} and on X_2 will give the constraints on a_{z4} . Finally, we use the

bounds on a_{z3} , a_{z2} and X_m to obtain constraints for $(a_m + \frac{1}{2}a_{ww2})$. Table 6 shows these results.

Bounds on X parameters	Bounds on anomalous coefficients
$-1.2 < X_3 < 0.5$	$-0.6 < a_{z2} < 0.32$
$-0.8 < X_4 < 1.3$	$-0.9 < a_{z3} < 1.1$
$03 < X_1 < .035$	$-0.17 < a_{zz1} < 0.15$
$-0.32 < X_2 < 0.82$	$-1.9 < a_{z4} < 1.7$
$28 < X_m < .12$	$-0.7 < a_m + \frac{1}{2}a_{ww2} < 0.4$

Table 6: The constraints on the anomalous coefficients obtained by the linear combination of the bounds on the X parameters.

Nevertheless, we can also follow the usual procedure of taking only one anomalous coefficient as non-zero at a time. Under this approach the bounds become more stringent:

$$\begin{array}{lll} -0.3 < & a_{zz1} & < 0.035 \; , \\ -0.28 < & a_m & < 0.12 \; , \\ -0.24 < & a_{z3} & < 0.28 \; , \\ -0.4 < & a_{z2} & < 0.2 \; , \\ -0.82 < & a_{ww2} & < 0.32 \; , \\ -0.56 < & a_{z4} & < 0.24 \; . \end{array} \tag{88}$$

Again, these bounds come from the consideration of a 2σ deviation from the no-Higgs SM event rates. For instance, at the LC, the no-Higgs SM predictions for the processes $Z_L Z_L \to t\bar{t}$ and $W_L^+ W_L^- \to t\bar{t}$ are 60 and 400, respectively [cf. Figs. 9 and 10]. This means that a number of events between 75 and 45 for the first process, and between 440 and 360 for the second one, is considered consistent with the no-Higgs SM prediction at the 95% C.L.. Fig. 9 shows an interesting situation for $Z_L Z_L \to t \bar{t}$, if the parameter X happened to be between 0.75 and 0.90 then we would obtain a number of events consistent with the no-Higgs SM. However, if this were the case, then X_1 would have to be at least of order 0.7 and we would observe a substantial deviation (of about 600) in the number of events produced from $W_L^+W_L^- \to t\bar{t}$. This also happens the other way around, if X_1 is between 0.38 and 0.45, we would obtain a production rate consistent with the no-Higgs SM for $W_L^+W_L^-$ fusion [cf. Fig. 10], but then X would be at least of order 0.3, and according to Fig. 9, we would observe only 18 $t\bar{t}$ pairs from $Z_L Z_L$ fusion, too far from the 60 ± 15 range of the no-Higgs SM prediction. Hence, all the production channels have to be measured to conclusively test the SM and probe new physics.

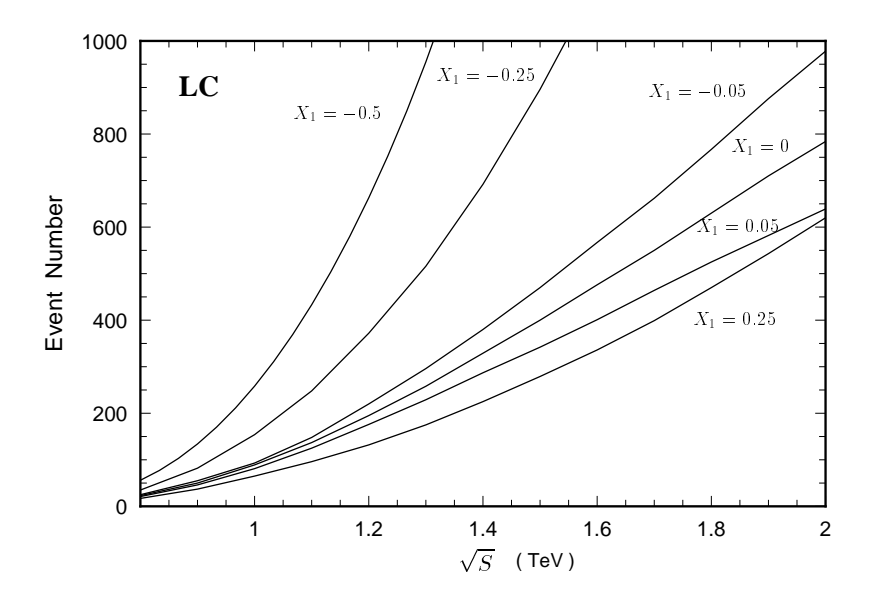


Figure 12: Number of $t\bar{t}$ events at the LC from $W_L^+W_L^-$ fusion for different values of the effective coefficient X_1 as a function of the CM energy.

The above results are for the LC with a 1.5 TeV CM energy. To study the possible new effects in the production rates of $W_L^+W_L^- \to t\bar{t}$ at the LC with different CM energies, we plot the production rates for various values of X_1 in Fig. 12. (Again, $X_1=0$ stands for the no-Higgs SM.) Notice that, if X_1 were as large as -0.5, then a 1 TeV LC could well observe the anomalous rate via $W_L^+W_L^-$ fusion. ²² For $X_1=0.25$ the event rate at 1.5 TeV is down by about a factor of 2 from the SM event rate. ²³

8.2 CP violating effects

The complete set of anomalous dimension 5 operators listed in $\mathcal{L}^{(5)}$ consists of operators with CP- conserving and non-conserving parts. In our study of the top quark production rates we have only considered the CP-even part of these operators; their contribution, like the one from the *no-Higss* SM at tree level, is real. However, a CP-odd operator can contribute to the imaginary part of the helicity amplitudes, and it can only be probed by examining CP-odd observables.

To illustrate this point, let us consider the CP-odd part of the four-point scalar type operator O_{gWW} and the electric dipole moment term of O_A [cf. Eqs. (54) and (59)]. After including contributions from the no-Higss SM and from the above two CP-odd operators, the helicity amplitudes for the $W_L^+W_L^- \to t\bar{t}$ process in the $W_L^+W_L^-$

 $^{^{22}\}mathrm{If}\ X_1$ is too big , partial wave unitarity can be violated at this order.

²³For positive values of X_1 the rate tends to diminish below the SM rate. However, near 0.25, the rate begins to rise again, toward the SM rate.

CM frame are:

$$T_{\pm\pm} = \pm \frac{m_t E}{v^2} + i2 \frac{E^3}{v^2} \frac{(\tilde{a}_{ww1} + 2a_d c_\theta)}{\Lambda} ,$$

$$T_{+-} = \frac{2 m_t^2 s_\theta}{\left(\frac{m_b^2}{2E^2} + (1 - c_\theta) \left(1 - \frac{m_t^2}{2E^2}\right)\right) v^2} ,$$

$$T_{-+} = 0 ,$$
(89)

where, by a_d and \tilde{a}_{ww1} , we refer to the imaginary part of the coefficients of O_A and O_{qWW} , respectively.

One of the CP-odd observables that can measure a_d and \tilde{a}_{ww1} is the transverse polarization (P_{\perp}) of the top quark, which is the degree of polarization of the top quark in the direction perpendicular to the plane of the $W_L^+W_L^- \to t\bar{t}$ scattering process. It was shown in Ref. [35] that

$$P_{\perp} = \frac{2Im\left(T_{++}^*T_{-+} + T_{+-}^*T_{--}\right)}{|ww_{++}|^2 + |ww_{+-}|^2 + |ww_{-+}|^2 + |ww_{--}|^2},\tag{90}$$

which, up to the order $\frac{1}{\Lambda}$, is

$$P_{\perp} \cong \frac{4s_{\theta}E}{\left(\frac{m_{b}^{2}}{2E^{2}} + (1 - c_{\theta})\left(1 - \frac{m_{t}^{2}}{2E^{2}}\right)\right)} \frac{(\tilde{a}_{ww1} + 2a_{d}c_{\theta})}{\Lambda}.$$
 (91)

Again, $E = \sqrt{s}$ is the CM energy of the $W_L^+W_L^-$ system; P_\perp , by definition, can only obtain values between -1 and 1. For E = 1.5 TeV, $\Lambda = 3$ TeV, and $\theta = \frac{\pi}{2}$, or $\frac{\pi}{3}$, we obtain $P_\perp = 4\tilde{a}_{ww1}$, or $4\sqrt{3}(\tilde{a}_{ww1} + a_d)$, respectively. Since $|P_\perp|$ is at most 1, this requires $|\tilde{a}_{ww1}| < \frac{1}{4}$ or $|\tilde{a}_{ww1} + a_d| < \frac{1}{4\sqrt{3}}$.

At a 1.5 TeV e^+e^- collider, the no-Higgs SM predicts about 100 $t\bar{t}$ pairs, with an invariant mass between 800 GeV and 1100 GeV, via the $W_L^+W_L^-$ fusion process . Let us assume that $a_d=0$, and that P_\perp can be measured to about $\frac{1}{\sqrt{100}}=10\%$, then an agreement between data and the no-Higgs SM prediction ($P_\perp=0$ at tree level) would imply $|\tilde{a}_{ww1}| \leq 0.04$.

9 Conclusions

If the fermion mass generation is closely related to the EWSB mechanism, one expects some residual effects of this mechanism to appear in accordance with the mass hierarchy. Since the mass of top quark is heavy, it is likely that the interactions of the top quark can deviate largely from the SM predictions. In this study, we have applied the electroweak chiral Lagrangian to probe new physics beyond the SM by studying

the couplings of the top quark to gauge bosons. We have restricted ourselves to only consider the interactions of the top and bottom quarks and not the flavor changing neutral currents that involve the other light quarks. Also, motivated by low energy data, we assume that the coupling of Z-b-b is not strongly modified by new physics.

In section 2, we introduced the dimension 4 non-linear chiral Lagrangian that contains the no-Higgs SM and the four unknown effective coefficients. Among them, two represent the non-standard couplings associated with the left- and right-handed charged currents κ_L^{CC} and κ_R^{CC} , and two more for the anomalous left- and right-handed neutral currents κ_L^{NC} and κ_R^{NC} . Constrains for these coefficients have been found using precision LEP/SLC data [4]. In particular, under the assumption that the b-b-Z vertex is not modified at tree level, κ_L^{NC} is bound within 0 and 0.15 (0.0 < κ_L^{NC} < 0.15). On the other hand, although κ_R^{NC} and κ_L^{CC} are allowed to vary in the full range of ± 1 , the precision LEP/SLC data do impose some correlations among κ_L^{NC} , κ_R^{NC} , and κ_L^{CC} . As for κ_R^{CC} , this coupling does not contribute to the LEP/SLC observables of interest in the limit of $m_b=0$, but it can be constrained independently by using the CLEO measurement of $b\to s\gamma$: $-0.037 < \kappa_R^{CC} < 0.0015$ [28, 29]. At the upgraded Tevatron (Run-II) and the LHC, κ_L^{CC} and κ_R^{CC} can be further tested by studying the production and the decay of the top quarks while κ_L^{NC} and κ_R^{NC} can be better measured at the LC.

If a strong dynamics of the electroweak symmetry breaking mechanism can largely modify the dimension 4 anomalous couplings, it is natural to ask whether the same dynamics can also give large dimension 5 anomalous couplings. In the framework of the electroweak chiral Lagrangian, we have found that there are 19 independent dimension five operators associated with the top quark and the bottom quark system. Their leading contributions to the helicity amplitudes for $V_L V_L \to t\bar{t}, t\bar{b}$, or $b\bar{t}$ processes are given in Appendices B and C. The high energy behavior of the above scattering processes due to the dimension 5 operators, two powers in E above the no-Higgs SM, provides a good opportunity to test these operators on the production of $t\bar{t}$ pairs or single-t or \bar{t} events in high energy collisions. Since, in the high energy regime, a longitudinal gauge boson is equivalent to the corresponding would-be Goldstone boson, the production of top quarks via $V_L V_L$ fusions shall probe the part of the electroweak symmetry breaking sector which modifies the top quark interactions. Since the dimension 4 anomalous couplings κ 's can be well measured at the scale of M_Z or m_t , we expect that their values will be already known by the time data is available for the study of $V_L V_L$ fusion processes in the TeV region. Hence, to simplify our discussion on the accuracy of the measurement of the dimension 5 anomalous couplings at future colliders, we have taken the dimension 4 anomalous couplings to be zero for this part of the study. Also we have considered a special class of new physics effects in which an underlying custodial SU(2) symmetry is assumed that

²⁴ We have used the updated data in Ref. [28] and the formula in Ref. [29] to recalculate this bound.

gets broken in such a way as to keep the couplings of the Z-b-b unaltered. This approximate custodial symmetry then relates some of the coefficients of the anomalous operators, reducing the number of independent coefficients from 19 down to 6 only. Then we study the contributions of these couplings to the production rates of the top quark at the LHC and the LC.

We find that for the leading contributions at high energies, only the S- and Ppartial wave amplitudes are modified by these anomalous couplings. If the magnitudes of the coefficients of the anomalous dimension 5 operators are allowed to be as large as 1 (as suggested by the naive dimensional analysis [25]), then we will be able to make an unmistakable identification of their effects to the production rates of top quarks via the longitudinal weak boson fusions. However, if the measurement of the top quark production rate is found to agree with the SM prediction, then one can bound these coefficients to be at most of order 10^{-1} . This is about a factor $\frac{\Lambda}{m_t} \simeq \frac{3\text{TeV}}{175\text{GeV}} \sim O(10)$ more stringent than in the case of the study of NLO bosonic operators via the $V_L V_L \to V_L V_L$ scattering processes [21, 31, 24]. Hence, for those models of electroweak symmetry breaking for which the naive dimensional analysis gives the correct size for the coefficients of dimension 5 effective operators, the top quark production via $V_L V_L$ fusions can be a more sensitive probe to EWSB than the longitudinal gauge boson pair production via $V_L V_L$ fusions which is commonly studied. For completeness, we also briefly discuss how to study the CP-odd operators by measuring CP-odd observables. In particular, we study their effects on the transverse (relative to the scattering plane of $W_L^+W_L^- \to t\bar{t}$) polarization of the top quark.

In conclusion, the production of top quarks via $V_L V_L$ fusions at the LHC and the LC should be carefully studied when data is available because it can be sensitive to the electroweak symmetry breaking mechanism, even more than the commonly studied $V_L V_L \rightarrow V_L V_L$ processes in some models of strong dynamics.

Acknowledgments

We thank Hong-Jian He, G. L. Kane, E. Malkawi and T. Tait for helpful discussions. F. Larios was supported in part by the Organization of American States, and by the Sistema Nacional de Investigadores. CPY was supported in part by the NSF grant No. PHY-9507683.

A Equations of Motion

From the electroweak chiral Lagrangian $\mathcal{L}^{(4)}$ of Eq. (33), we can use the Euler-Lagrange equations to obtain the equations of motion for the top quark. They are:

$$i\gamma^{\mu}(\partial_{\mu} + i\frac{2}{3}s_{w}^{2}\mathcal{A}_{\mu})t_{L} - \frac{1}{2}(1 - \frac{4}{3}s_{w}^{2} + \kappa_{L}^{NC})\gamma^{\mu}\mathcal{Z}_{\mu}t_{L} - \frac{1}{\sqrt{2}}(1 + \kappa_{L}^{CC})\gamma^{\mu}\mathcal{W}_{\mu}^{+}b_{L} - m_{t}t_{R} = 0,$$

$$i\gamma^{\mu}(\partial_{\mu} + i\frac{2}{3}s_{w}^{2}\mathcal{A}_{\mu})t_{R} - \frac{1}{2}(-\frac{4}{3}s_{w}^{2} + \kappa_{R}^{NC})\gamma^{\mu}\mathcal{Z}_{\mu}t_{R} - \frac{1}{\sqrt{2}}\kappa_{R}^{CC}\gamma^{\mu}\mathcal{W}_{\mu}^{+}b_{R} - m_{t}t_{L} = 0,$$

$$i\gamma^{\mu}(\partial_{\mu} - i\frac{1}{3}s_{w}^{2}\mathcal{A}_{\mu})b_{L} - (-\frac{1}{2} + \frac{1}{3}s_{w}^{2})\gamma^{\mu}\mathcal{Z}_{\mu}b_{L} - \frac{1}{\sqrt{2}}(1 + \kappa_{L}^{CC\dagger})\gamma^{\mu}\mathcal{W}_{\mu}^{-}t_{L} - m_{b}b_{R} = 0,$$

$$i\gamma^{\mu}(\partial_{\mu} - i\frac{1}{3}s_{w}^{2}\mathcal{A}_{\mu})b_{R} - \frac{1}{3}s_{w}^{2}\gamma^{\mu}\mathcal{Z}_{\mu}b_{R} - \frac{1}{\sqrt{2}}\kappa_{R}^{CC\dagger}\gamma^{\mu}\mathcal{W}_{\mu}^{-}t_{R} - m_{b}b_{L} = 0.$$

${f B} \quad {\cal L}^{(4)} \,\, { m helicity} \,\, { m amplitudes}$

Below, we show the leading contributions in powers of E (the CM energy of the $V_L V_L$ system) of the helicity amplitudes for the processes $V_L V_L \to t\bar{t}$, $t\bar{b}$ and $b\bar{t}$, in the limit $E \gg m_t \gg m_b$, and for the no-Higgs SM (i.e. $\mathcal{L}_{SM}^{(4)}$).²⁵ In general, any contribution that is not proportional to E^3 or $m_t E^2$ (the highest leading factors) is neglected throughout this paper.

B.1
$$Z_L Z_L \to t \overline{t}$$
 and $W_L^+ W_L^- \to t \overline{t}$

The helicity amplitudes for $t\bar{t}$ production are given as follows. The first two letters, zz or ww, refer to the $Z_LZ_L\to t\bar{t}$ or $W_L^+W_L^-\to t\bar{t}$ scattering processes, respectively. The first and second adjacent symbols (+ or -), refer to the helicities of the final top and anti-top quarks, respectively. Throughout this paper, the scattering angle θ is defined as the one subtended between the momentum of the incoming gauge boson that appears on the top-left part of the Feynman diagram [cf. Figs. 3, 4 and 5] and the momentum of the outgoing fermion appearing on the top-right part of the same diagram; all in the CM frame of the V_LV_L pair. We denote its sine and cosine functions as s_θ and c_θ , respectively.

$$zz_{++} = -zz_{--} = \frac{m_t E}{v^2},$$

$$zz_{+-} = zz_{-+} = \frac{2 m_t^2 c_\theta s_\theta}{\left(\frac{4c_\theta^2 m_t^2}{E^2} + s_\theta^2\right) v^2},$$

$$ww_{++} = -ww_{--} = zz_{++},$$

 $^{^{25}}$ These amplitudes agree with those given in Ref. [36].

$$ww_{+-} = \frac{2 m_t^2 s_\theta}{\left(\frac{2m_b^2}{E^2} + (1 - c_\theta) \left(1 - \frac{2m_t^2}{E^2}\right)\right) v^2},$$

$$ww_{-+} = \frac{2 m_b^2 s_\theta}{\left(\frac{2m_b^2}{E^2} + (1 - c_\theta) \left(1 - \frac{2m_t^2}{E^2}\right)\right) v^2}.$$
(B.1)

For ww_{+-} we have kept the term proportional to the b-mass in the denominator of the fermion-propagator to avoid infinities at $\theta = 0$ in the numerical computations.

For completeness, we include the leading contributions that may come from the κ coefficients in $\mathcal{L}^{(4)}$ [cf. Eq. (33)]:

$$zz_{++}^{\kappa} = -zz_{--}^{\kappa} = \frac{m_t E}{v^2} \left[(\kappa_L^{NC} - \kappa_R^{NC} + 1)^2 - 1 \right] ,$$

$$zz_{+-}^{\kappa} = zz_{-+}^{\kappa} = \frac{2 m_t^2 c_{\theta} s_{\theta}}{\left(\frac{4c_{\theta}^2 m_t^2}{E^2} + s_{\theta}^2 \right) v^2} \left[(\kappa_L^{NC} - \kappa_R^{NC} + 1)^2 - 1 \right] ,$$

$$ww_{++}^{\kappa} = \frac{m_t E}{v^2} \left[(1 + c_{\theta}) (2\kappa_L^{CC} + (\kappa_L^{CC})^2 + (\kappa_R^{CC})^2) - c_{\theta} (\kappa_L^{NC} + \kappa_R^{NC}) \right] ,$$

$$ww_{--}^{\kappa} = -ww_{++}^{\kappa}$$

$$ww_{+-}^{\kappa} = \frac{E^2 s_{\theta}}{v^2} \left[\kappa_R^{NC} - (\kappa_R^{CC})^2 \right] ,$$

$$ww_{-+}^{\kappa} = \frac{E^2 s_{\theta}}{v^2} \left[\kappa_L^{NC} - \kappa_L^{CC} (2 + \kappa_L^{CC}) \right] .$$

$$(B.2)$$

B.2 $W_L^+ Z_L \to t \overline{b}$ and $W_L^- Z_L \to b \overline{t}$

The following helicity amplitudes for single top or anti-top production were not given in Ref. [36]. We have taken the limit $E \gg m_t \gg m_b$. The first three letters, wzt or wzb, refer to the $W_L^+Z_L \to t\overline{b}$ or $W_L^-Z_L \to b\overline{t}$ scattering process, respectively.

$$\begin{split} wzt_{++} &= & -\frac{\sqrt{2} \, m_t^3 \, \left(1-c_\theta\right)}{E \left(1-\frac{2m_t^2}{E^2}\right) \, \left(1+c_\theta+\frac{2m_t^2}{E^2}\right) \, v^2} \,, \\ wzt_{--} &= & 0 \,, \\ wzt_{+-} &= & 0 \,, \\ wzt_{-+} &= & -\frac{\sqrt{2} \, m_t^2 \, s_\theta}{\left(1-\frac{2m_t^2}{E^2}\right) \left(1+c_\theta+\frac{2m_t^2}{E^2}\right) v^2} \,, \\ wzb_{++} &= & -wzt_{--}(c_\theta\to-c_\theta) \,=\, 0 \,, \\ wzb_{--} &= & -wzt_{++}(c_\theta\to-c_\theta) \,=\, \frac{\sqrt{2} \, m_t^3 \, \left(1+c_\theta\right)}{E \left(1-\frac{2m_t^2}{E^2}\right) \left(1-c_\theta+\frac{2m_t^2}{E^2}\right) v^2} \\ wzb_{-+} &= & -wzt_{-+}(c_\theta\to-c_\theta) \,=\, \frac{\sqrt{2} \, m_t^3 \, \left(1-c_\theta+\frac{2m_t^2}{E^2}\right) v^2}{\left(1-\frac{2m_t^2}{E^2}\right) \left(1-c_\theta+\frac{2m_t^2}{E^2}\right) v^2} \,, \end{split}$$

$$wzb_{+-} = -wzt_{+-}(c_{\theta} \to -c_{\theta}) = 0.$$
 (B.3)

Including the contributions from the κ coefficients in $\mathcal{L}^{(4)}$, we obtain:

$$wzt_{++}^{\kappa} = \frac{E m_{t}}{v^{2}\sqrt{2}} (1 + \kappa_{L}^{CC}) \left[(1 - c_{\theta})\kappa_{L}^{NC} - 2\kappa_{R}^{NC} \right] ,$$

$$wzt_{--}^{\kappa} = \frac{E m_{t}}{v^{2}\sqrt{2}} \kappa_{R}^{CC} \left[2\kappa_{L}^{NC} + (1 - c_{\theta})(2 - \kappa_{R}^{NC}) \right] ,$$

$$wzt_{+-}^{\kappa} = \frac{E^{2}s_{\theta}}{v^{2}\sqrt{2}} \kappa_{R}^{CC} \left(\kappa_{R}^{NC} - 2 \right) ,$$

$$wzt_{-+}^{\kappa} = \frac{E^{2}s_{\theta}}{v^{2}\sqrt{2}} \kappa_{L}^{NC} \left(1 + \kappa_{L}^{CC} \right) . \tag{B.4}$$

${f C} \quad {\cal L}^{(5)} \,\, { m helicity} \,\, { m amplitudes}$

Below, we show the anomalous coupling contributions to the helicity amplitudes for the $V_L V_L \to t\bar{t}$, $t\bar{b}$ or $b\bar{t}$ scattering processes. The first letter, a, stands for anomalous. All the 19 anomalous operators listed in section 4 have been considered.

C.1 $Z_L Z_L \rightarrow t \overline{t}$

There are four operators relevant to this process. The four-point operator O_{gZZ} , with coefficient a_{zz1} , contributes only through the diagram of Fig. 3(c). The other three, $O_{\sigma DZ}$, O_{ZDf} and O_{gDZ} , with coefficients a_{z2} , a_{z3} and a_{z4} , respectively, contribute through diagrams 3(a) and 3(b). However, since external on-shell Z bosons satisfy the condition $p_{\mu}\epsilon^{\mu}=0$, the contribution from the derivative-on-boson operators $O_{\sigma DZ}$ and O_{gDZ} vanishes. The only non-zero contributions come from O_{gZZ} and O_{ZDf} . The anomalous contributions to the helicity amplitudes are:

$$azz_{++} = \frac{-E^3 \left(2 a_{zz1} + \left(1 - \frac{8}{3} s_w^2\right) a_{z3}\right)}{v^2 \Lambda},$$

$$azz_{--} = -azz_{++},$$

$$azz_{+-} = az_{-+} = 0,$$
(C.1)

The amplitudes with opposite sign helicities azz_{+-} and azz_{-+} appear as zero. This is so because the contribution from the four-point operator $O_{g\mathcal{Z}\mathcal{Z}}$ is proportional to the spinor product $\overline{u}[\lambda=\pm 1]v[\lambda=\mp 1]$, which is zero in the CM frame of the $t\overline{t}$ pair. Furthermore, for the operator with derivative-on-fermion, $O_{\mathcal{Z}Df}$, the leading energy power for $azz_{\pm\mp}$ is E^0 and we do not include it in the above results.

C.2 $W_L^+W_L^- \to t\bar{t}$

The relevant operators are: the four-point operators O_{gWW} and $O_{\sigma WW}$ with coefficients a_{ww1} and a_{ww2} , respectively; derivative-on-boson operators $O_{\sigma DZ}$, O_{gDZ} , $O_{\sigma DWL(R)}$, $O_{gDWL(R)}$ and O_{A} , with coefficients a_{z2} , a_{z4} , $a_{w2L(R)}$, $a_{w4L(R)}$ and a_{m} , respectively; derivative-on-fermion operators O_{ZDf} , $O_{WDtR(L)}$ and $O_{WDbL(R)}$, with coefficients a_{z3} , $a_{w3R(L)}$ and $a_{bw3L(R)}$, respectively.

However, some operators give null contributions. For instance, $a_{w2L(R)}$ and $a_{w4L(R)}$ enter in the t-channel diagram of Fig. 4(a), but the condition $\epsilon_{\mu}p^{\mu}=0$ for the on-shell W^+ and W^- bosons makes their contribution to vanish. Similarly, the contribution from O_{gWW} is proportional to the spinor product $\overline{u}[\lambda=\pm 1]v[\lambda=\mp 1]$, which is zero in the $t\overline{t}$ CM frame; also, the contribution from O_{gDZ} , which enters in the s-channel diagram 4(c), vanishes when the Lorentz contraction in the product of the tri-boson coupling, the bosonic propagator and the anomalous coupling is done. There is no effect from operators that depend on b_R , such as O_{gDWL} , O_{WDtL} and O_{WDbL} , because the bottom quark is purely left handed in diagram 4(a) in the limit $m_b \to 0$. Also, the contributions from the operators $O_{WDtR(L)}$ (with coefficient $a_{w3R(L)}$) and $O_{WDbL(R)}$ (with coefficient $a_{bw3L(R)}$) are identical. Hence, the helicity amplitudes are:

$$aww_{++} = -\frac{2E^{3}}{v^{2}\Lambda} \left(a_{ww1} + a_{ww2} c_{\theta} \right) - \frac{E^{3}}{v^{2}\Lambda} \left(\frac{a_{w3R} + a_{bw3R}}{\sqrt{2}} + c_{\theta} \left(-\frac{a_{w3R} + a_{bw3R}}{\sqrt{2}} - 2 a_{z2} + a_{z3} + 4 a_{m} \right) \right) ,$$

$$aww_{--} = -aww_{++} ,$$

$$aww_{+-} = \frac{2E^{2} m_{t} s_{\theta}}{v^{2}\Lambda} \left(2 a_{ww2} - \frac{a_{w3R} + a_{bw3R}}{\sqrt{2}} - 2 a_{z2} + 4 a_{m} \right) ,$$

$$aww_{-+} = \frac{2E^{2} m_{t} s_{\theta}}{v^{2}\Lambda} \left(2 a_{ww2} - 2 a_{z2} + 4 a_{m} \right) . \tag{C.2}$$

$\mathbf{C.3} \qquad W_L^+ Z_L \to t \overline{b}$

There are two kinds of operators that contribute to this process. The first ones (operators with top and bottom quarks) distinguish chirality; the second ones (operators with top quarks only) do not. The ones that distinguish chirality are: the four-point operators $O_{gWZL(R)}$ and $O_{\sigma WZL(R)}$, with coefficients $a_{wz1L(R)}$ and $a_{wz2L(R)}$, respectively; derivative-on-boson operators $O_{\sigma DWL(R)}$ and $O_{gDWL(R)}$, with coefficients $a_{w2L(R)}$ and $a_{w3L(R)}$, respectively; derivative-on-fermion operators $O_{WDtR(L)}$ and $O_{WDbL(R)}$, with coefficients $a_{w3R(L)}$ and $a_{bw3L(R)}$, respectively. The second ones, that do not distinguish chirality, are: derivative-on-boson operators $O_{\sigma DZ}$ and O_{gDZ} , with coefficients a_{z2} and a_{z4} , respectively; derivative-on-fermion operator O_{ZDf} , with coefficient a_{z3} .

A particular feature, common to all the operators that distinguish chirality, takes

place: If the helicity of the particle is *opposite* to the chirality in the coupling, then the contribution will be proportional to the mass of that particle. For instance, the leading term for the contribution of O_{WDtR} to $awzt_{++}$ is proportional to E^3 , but the leading term for $awzt_{--}$ is proportional to $m_tm_bE^1$. (The left handed helicity of the anti-bottom is *opposite* to its left handed chiral component.)

The three relevant operators that do not distinguish chirality participate only through the *u-channel* diagram of Fig. 5(b), and only O_{ZDf} gives non-zero contribution. The other two, with derivative on boson, have their contribution vanished from the condition $\epsilon_{\mu}p^{\mu}=0$ of the on-shell Z boson. On the other hand, the contribution of O_{ZDf} to those amplitudes with a left handed helicity anti-bottom is zero in the limit $m_b \to 0$ because the bottom becomes purely left handed in this diagram. Hence,

$$awzt_{++} = \frac{E^{3}}{2v^{2}\Lambda} \left(a_{w3R} + a_{bw3R} \left(1 + \frac{2}{3} s_{w}^{2} + c_{\theta} \right) - 4 a_{wz1R} - 4 a_{wz2R} c_{\theta} - \sqrt{2} a_{z3} \left(1 + c_{\theta} \right) - 4 c_{w}^{2} a_{w2R} c_{\theta} + 4 s_{w}^{2} a_{w4R} \right) ,$$

$$awzt_{+-} = \frac{E^{2} m_{t} s_{\theta}}{2v^{2}\Lambda} \left(4 a_{wz2L} + a_{w3L} + a_{bw3L} + 4 c_{w}^{2} a_{w2L} \right) ,$$

$$awzt_{-+} = \frac{E^{2} m_{t} s_{\theta}}{2v^{2}\Lambda} \left(4 a_{wz2R} - a_{w3R} + a_{bw3R} - \sqrt{2} a_{z3} + 4 c_{w}^{2} a_{w2R} \right) ,$$

$$awzt_{--} = \frac{E^{3}}{2v^{2}\Lambda} \left(4 a_{wz1L} + 4 a_{wz2L} c_{\theta} + 4 c_{w}^{2} a_{w2L} c_{\theta} + a_{wz2L} c_{\theta} + 4 c_{w}^{2} a_{w4L} \right) ,$$

$$(C.3)$$

C.4 $W_L^- Z_L \to b \overline{t}$

This process is similar to $W_L^+ Z_L \to t\bar{b}$, as discussed above. The same kind of operators contribute here, and the same reasons of why some contributions are negligible or zero apply.

$$awzb_{++} = -awzt_{--} (c_{\theta} \to -c_{\theta})$$

$$= \frac{E^{3}}{2v^{2}\Lambda} \left(-4 a_{wz1L} + 4 a_{wz2L} c_{\theta} + 4 c_{w}^{2} a_{w2L} c_{\theta} - a_{w3L} + a_{bw3L} \left(1 - \frac{2}{3} s_{w}^{2} + c_{\theta} \right) + 4 s_{w}^{2} a_{w4L} \right) ,$$

$$awzb_{--} = -awzt_{++} (c_{\theta} \to -c_{\theta})$$

$$= \frac{E^{3}}{2v^{2}\Lambda} \left(4 a_{wz1R} + \sqrt{2} a_{z3} \left(1 - c_{\theta} \right) - a_{wz2R} c_{\theta} - 4 c_{w}^{2} a_{w2R} c_{\theta} - a_{w3R} + a_{bw3R} \left(1 + \frac{2}{3} s_{w}^{2} - c_{\theta} \right) - 4 s_{w}^{2} a_{w4R} \right) ,$$

$$awzb_{+-} = -awzt_{+-} ,$$

$$awzb_{-+} = -awzt_{-+} . \tag{C.4}$$

References

- F. Abe et al., Phys. Rev. Lett. 73, 225 (1994);
 S. Abachi et al., Phys. Rev. Lett. 72, 2138 (1994);
 CDF Collaboration, Phys. Rev. Lett. 74, 2626 (1995);
 D0 Collaboration, Phys. Rev. Lett. 74, 2632 (1995);
 L. Roberts, to appear in the Proceedings of the 28th International Conference on High Energy Physics, Warsaw, Poland, 1996.
- R.D. Peccei and X. Zhang, Nucl. Phys. B337, 269 (1990);
 R.D. Peccei, S. Peris and X. Zhang, Nucl. Phys. B349, 305 (1990).
- [3] R.S. Chivukula, E. Gates, E.H. Simmons and J. Terning, Phys. Lett. B311, 157 (1993);
 R.S. Chivukula, E.H. Simmons and J. Terning, Phys. Lett. B331, 383 (1994).
- [4] D.O. Carlson, E. Malkawi, C.-P. Yuan, Phys. Lett. B337 145 (1994);
 E. Malkawi and C.-P. Yuan. Phys. Rev. D50, 4462 (1994); and Phys. Rev. D52, 472 (1995);
 E. Malkawi Ph. D. Thesis, Michigan State University, August 1996.
 - E. Malkawi, Ph.D. Thesis, Michigan State University, August 1996; E. Malkawi, T. Tait, C.-P. Yuan, Phys. Lett. **B385**, 304 (1996).
- [5] G.L. Kane, published in Proceedings of the Workshop on High Energy Phenomenology, Mexico City, July 1–10, 1991.
- [6] H. Georgi, "Effective Field Theory", in Annu. Rev. Nucl. Part. Sci. 43, 209 (1993).
- [7] For instance, see, R. Martinez, M.A. Perez and J.J. Toscano, Phys. Lett. B340, 91 (1994);
 M.A. Perez, J.J. Toscano and J. Wudka, Phys. Rev. D52, 494 (1995).
- [8] S. Coleman, J. Wess and B. Zumino, Phys. Rev. **D177**, 2239 (1969);
 C.G. Callan, S. Coleman, J. Wess and B. Zumino, Phys. Rev. **D177**, 2247 (1969);
 S. Weinberg, Physica **96A**, 327 (1979).
- [9] S. Dawson, Nucl. Phys. **B249**, 42 (1985).
- [10] S. Dawson and S. Willenbrock, Nucl. Phys. **B284**, 449 (1987);
 S. Willenbrock and D.A. Dicus, Phys. Rev. **D34**, 155 (1986).
- [11] C.-P. Yuan, Phys. Rev. D41, 42 (1990);
 T. Moers, R. Priem, D. Rein and H. Reithler, in *Proceedings of Large Hadron Collider Workshop*, preprint CERN 90-10, 1990;

- F. Anselmo, B. van Eijk and G. Bordes, Phys. Rev. **D45**, 2312 (1992);
- S. Mrenna and C.–P. Yuan, Phys. Rev. **D46**, 1007 (1992);
- R.K. Ellis and S. Parke, Phys. Rev. **D46**, 3785 (1992);
- D.O. Carlson and C.-P. Yuan, Phys. Lett. **B306**, 386 (1993);
- D.O. Carlson, Ph.D. thesis, Michigan State University, MSUHEP-050727, hep-ph/9508278;
- A.P. Heinson, A.S. Belyaev and E. Boos, hep-ph/9509274, Presented at Workshop on Physics of the Top Quark, Ames, IA, 25-26 May 1995; and hep-ph/9612424.
- [12] C.-P. Yuan, published in Proc. of Workshops on Particles and Fields and Phenomenology of Fundamental Interactions, Puebla, Mexico, Nov. 1995;
 D.O. Carlson and C.-P. Yuan, hep-ph/9509208, Presented at Workshop on Physics of the Top Quark, Ames, IA, May 25-26, 1995.
- [13] G. Bordes, B. van Eijk, Nucl. Phys. **B435**, 23 (1995).
- [14] S. Cortese and R. Petronzio, Phys. Lett. B253, 494 (1991);
 T. Stelzer and S. Willenbrock, Phys. Lett. B374, 169 (1996);
 Future Electroweak Physics at the Fermilab Tevatron, Report of the tev_2000 study group, Eds. D. Amidei and R. Brock, Fermilab-Pub-96/082 (1996).
- [15] M. Smith and S. Willenbrock, Phys. Rev. **D54**, 6696 (1996).
- [16] E. Boos, Y. Kurihara, Y. Shimizu, M. Sachwitz, H.J. Schreiber, S. Shichanin, Z. Phys. C70, 255 (1996).
- [17] G.A. Ladinsky and C.-P. Yuan, Phys. Rev. **D49**, 4415 (1994).
- [18] J.M. Cornwall, D.N. Levin, and G. Tiktopoulos, Phys. Rev. D10, 1145 (1974);
 C.E. Vayonakis, Lett. Nuovo. Cimento 17, 383 (1976);
 B.W. Lee, C. Quigg, and H. Thacker, Phys. Rev. D16, 1519 (1977);
 M.S. Chanowitz and M.K. Gaillard, Nucl. Phys. B261, 379 (1985);
 G.J. Gounaris, R. Kögerler, and H. Neufeld, Phys. Rev. D34, 3257 (1986);
 H. Veltman, *ibid*, D41 2294 (1990);
 W.B. Kilgore, Phys. Lett. B294, 257 (1992).
- [19] Y.-P. Yao and C.-P. Yuan, Phys. Rev. **D38**, 2237 (1988);
 J. Bagger and C. Schmidt, Phys. Rev. **D41**, 264 (1990).
- [20] H.-J. He, Y.-P. Kuang, and X. Li, Phys. Rev. Lett. 69, 2619 (1992);
 Phys. Rev. D49, 4842 (1994); Phys. Lett. B329, 278 (1994);
 H.-J. He and W.B. Kilgore, hep-ph/9609326 (Phys. Rev. D, in press).

- [21] H.-J. He, Y.-P. Kuang, and C.-P. Yuan, Phys. Rev. D51, 6463 (1995); hep-ph/9503359, Published in Proc. International Symposium on Beyond The Standard Model IV, Eds. J.F. Gunion, T. Han, J. Ohnemus, December 13-18, 1994, Tahoe, California, USA.
- [22] T. Han, R.D. Peccei and X. Zhang, Nucl. Phys. B454, 527 (1995);
 T. Han, K. Whisnant, B.L. Young, X. Zhang, hep-ph/9603247, 1996.
- [23] E. Malkawi and T. Tait, Phys. Rev. **D54**, 5758 (1996);
 Tim Tait, C.-P. Yuan, hep-ph/9611244, 1996.
- [24] J. Bagger, V. Barger, K. Cheung, J. Gunion, T. Han, G.A. Ladinsky, R. Rosenfeld, and C.-P. Yuan, Phys. Rev. **D49**, 1246 (1994); and **D52**, 3878 (1995).
 V. Barger, J. F. Beacom, K. Cheung, T. Han, Phys. Rev. **D50**, 6704 (1993).
- [25] H. Georgi, Weak Interactions and Modern Particle Theory (The Benjamin/Cummings Publishing Company, 1984);
 A. Manohar and H. Georgi, Nucl. Phys. B234, 189 (1984).
- [26] M. Chanowitz, M. Golden, and H. Georgi. Phys. Rev. **D36**, 1490 (1987);
 F. Feruglio, Int. J. Mod. Phys. **A8**, 4937 (1993).
- [27] T. Appelquist and C. Bernard, Phys. Rev. **D22**, 200 (1980); A.C. Longhitano,
 Nucl. Phys. **B188**, 118 (1981); T. Appelquist and G.-H. Wu, Phys. Rev. **D48**,
 3235 (1993); **D51**, 240 (1995); and references therein.
- [28] M. Alam et al., CLEO collaboration, Phys. Rev. Lett. 74 (1995) 2885.
- [29] K. Fujikawa and A. Yamada, Phys. Rev. **D49**, 5890 (1994).
- [30] W. Buchmüller and D. Wyler, Nucl. Phys. **B268**, 621 (1986).
- [31] H.-J. He, Y.-P. Kuang and C.-P. Yuan, Phys. Lett. B382, 149 (1996); and hep-ph/9611316, to appear in Phys. Rev. D, (1997); and MSUHEP-51201, Published in Proc. of International Workshop on Physics and Experiments with Linear Colliders, September 8-12, 1995, Iwate, Japan.
- [32] See, for example, J.F. Donogue, E. Golowich and B.R. Holstein, *Dynamics of the Standard Model* Cambridge monographs on particle physics, nuclear physics and cosmology. Cambridge University Press (1992).
- [33] R. N. Cahn and S. Dawson, Phys. Lett. B136, 196 (1984), Phys. Lett. B138, 464(E) (1984);
 M. S. Chanowitz and M. K. Gaillard, Phys. Lett. B142, 85 (1984);
 C. L. Kana, W. W. Barka and W. B. Balvick, Phys. Lett. B148, 267 (1984).
 - G. L. Kane, W. W. Repko and W. R. Rolnick, Phys. Lett. **B148**, 367 (1984);

- J. Lindfors, Z. Phys. C28, 427 (1985);
- W. B. Rolnick, Nucl. Phys. **B274**, 171 (1986);
- P. W. Johnson, F. I. Olness and W.-K. Tung, Phys. Rev. **D36**, 291 (1987);
- Z. Kunszt and D. E. Soper, Nucl. Phys. **B296**, 253 (1988);
- A. Abbasabadi, W. W. Repko, D. A. Dicus and R. Vega, Phys. Rev. **D38**, 2770 (1988);
- S. Dawson, Phys. Lett. **B217**, 347 (1989);
- S. Cortese and R. Petronzio, Phys. Lett. **B276**, 203 (1992);
- I. Kuss and H. Spiesberger, Phys. Rev. **D53**, 6078 (1996).
- [34] H.L. Lai, J. Botts, J. Huston, J.G. Morfin, J.F. Owens, J.W. Qiu, W.K. Tung, H. Weerts, Phys. Rev. **D51**, 4763 (1995).
- [35] G.L. Kane, G.A. Ladinsky and C.-P. Yuan, Phys. Rev. **D45**, 124 (1992).
- [36] M.S. Chanowitz, M.A. Furman and I. Hinchliffe, Nucl. Phys. **B153**, 402 (1979).